NACA

$N63-13877$

Code 1

RESEARCH MEMORANDUM

AN ANALOG STUDY OF THE INFLUENCE OF INTERNAL MODIFICATIONS

TO A WING LEADING EDGE ON ITS TRANSIENT TEMPERATURE

RISE DURING HIGH-SPEED FLIGHT

By Carr B. Neel

Ames Aeronautical Laboratory
Moffett Field, Calif.

OTS PRICE

XEROX $ _____

MICROFILM $ _____

NATIONAL ADVISORY COMMITTEE
FOR AERONAUTICS
WASHINGTON
March 17, 1958

UNCLASSIFIED

NATIONAL ADVISORY COMMITTEE FOR AERONAUTICS

RESEARCH MEMORANDUM

AN ANALOG STUDY OF THE INFLUENCE OF INTERNAL MODIFICATIONS

TO A WING LEADING EDGE ON ITS TRANSIENT TEMPERATURE

RISE DURING HIGH-SPEED FLIGHT
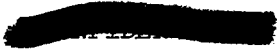
By Carr B. Neel

SUMMARY

An investigation was made with an electrical heat-flow analog to determine the effect of internal modifications to a wing leading edge on the surface-temperature rise and temperature distribution for conditions of transient aerodynamic heating at high supersonic speeds.

The study showed that when heat-absorbing material is concentrated in the wing leading-edge region, in the case of wings of large leading-edge radius, the temperature rise at the leading-edge point is determined primarily by the specific heat of the material. As the leading-edge radius is decreased, the thermal conductivity of the heat-absorbing material was shown to have an increasingly important effect. For cases of wings in which the skin is of uniform thickness in the leading-edge region, thermal conduction is of major importance in restricting the leading-edge temperature rise.

Because of its high specific heat and thermal conductivity, beryllium appears attractive in heat-sink applications. In an example, beryllium was shown to be far superior to Inconel-X from the standpoints of leading-edge-temperature rise, temperature distribution, and weight.

INTRODUCTION

During high-speed flight, the temperature rise of wing leading edges may become critical because of the high rates of local heat transfer. If the duration of flight is sufficiently short, the thermal capacity of the leading-edge material can be used as a heat sink to absorb the incoming heat and restrict the temperature rise to tolerable limits. The temperature rise depends in part on the mass and distribution of the heat-absorbing material, its specific heat and thermal conductivity, and the duration of flight. A comparison of the effectiveness of various heat-sink materials in limiting the temperature of high-speed body noses is given in reference 1.

In order to investigate the influence of modifying the internal structure of a high-speed wing leading edge on its temperature rise, calculations were performed on the Ames electrical heat-flow analog to determine the time-temperature histories and surface-temperature distributions of the leading-edge region with various internal arrangements of several metals for a particular flight trajectory. The trajectory encompassed speeds up to a Mach number of 6.5 and altitudes up to approximately 130,000 feet.

This report presents the results of the analog calculations and a brief analysis to indicate the relative importance of thermal conductivity and thermal capacity in lowering the surface temperature.

EQUATION OF HEAT FLOW AT WING SURFACE

The temperature rise of an element of wing skin is influenced by convective heat transfer, thermal capacity of the skin, conductive heat exchange, and radiant heat loss. Consider an element of wing skin with surface area dx dy and thickness dz which is subject to convective heating. Neglecting solar and nocturnal irradiation, the following expressions govern the temperature rise of the element:

Rate of convective heat flow into element $= h \, dx \, dy \left(T_r - T_w \right)$

Rate of heat storage in element $= \rho c_p \, dx \, dy \, dz \, \dfrac{\partial T_w}{\partial \theta}$

Rate of heat removal by conduction $= -k \left(\dfrac{\partial^2 T_w}{\partial x^2} + \dfrac{\partial^2 T_w}{\partial y^2} + \dfrac{\partial^2 T_w}{\partial z^2} \right) dx \, dy \, dz$

Rate of heat loss by radiation $= \sigma \epsilon \, dx \, dy \, T_w^{\,4}$

When the rate of heat flow into the element is equated to the heat being removed and stored, the following equation is derived:

$$h\left(T_r - T_w\right) = \rho c_p \frac{\partial T_w}{\partial \theta} \, dz - k\left(\frac{\partial^2 T_w}{\partial x^2} + \frac{\partial^2 T_w}{\partial y^2} + \frac{\partial^2 T_w}{\partial z^2}\right) dz + \sigma \epsilon T_w^{\,4} \qquad (1)$$

where

c_p specific heat of wing material, Btu/lb °F

h convective heat-transfer coefficient, Btu/hr ft² °F

k　　thermal conductivity of wing material, Btu/hr ft^2 ^{O}F/ft

T_r　　recovery temperature of boundary layer, ^{O}R

T_w　　temperature at surface of element, ^{O}R

ϵ　　radiative emissivity of the surface, dimensionless

ρ　　density of wing material, lb/ft^3

σ　　Stefan-Boltzmann constant, 0.173×10^{-8} Btu/hr ft^2 ^{O}R^4

θ　　time, hr

　　　In this investigation, it was assumed that spanwise heat flow was negligible. Hence, in the electrical-analog solutions, equation (1) was reduced to the two-dimensional case, involving only the coordinate variables x and z.

DESCRIPTION OF ELECTRICAL HEAT-FLOW ANALOG

　　　The Ames electrical heat-flow analog employs the analogy between the flow of heat and the flow of electricity. In the analogy, electrical current flow represents heat flow, voltage represents temperature, electrical resistance represents thermal resistance, and electrical capacitance represents thermal capacitance. When resistances and capacitances are connected in a circuit representative of the thermal circuit of a body, and electrical input functions are programmed to simulate the external heating conditions, the resultant current flows and voltages in the system are directly analogous to the heat flows and temperatures which would prevail in the body. The distribution of temperature and absorption of heat throughout the structure are accurately represented in the electrical circuit. The electrical analogy is discussed in greater detail in references 2 to 5.

　　　The analog consists of a resistance-capacitance network for simulating the thermal circuit of the body under investigation, the input-function-generating equipment for simulating the external heating conditions, and the recording system. Each of these components will be described.

Resistance-Capacitance Network

　　　The resistances of the resistance-capacitance network consist of potentiometers connected as rheostats, while the capacitances consist of condensers which can be plugged in to obtain the desired values. The network is shown in figure 1(a).

In the application of the analog to the leading-edge problem, the wing was divided into a number of small segments, and the thermal capacity of each of the segments and the thermal resistances between segments were determined. These values were converted into equivalent electrical terms, and the electrical circuit was set up on the analog. This circuit, then, represented the capacitive and conductive terms given in equation (1).

Input-Generating Equipment

The input equipment is used for generating the appropriate boundary conditions and provides, in equivalent electrical terms, the conditions required to simulate the recovery temperatures in the boundary layer, the convective heat-transfer coefficients, and the radiant heat loss from the surface. Since the recovery temperatures and heat-transfer coefficients over the surface vary with time, a switching system is employed to provide a stepwise variation of these parameters. The input equipment is shown in figure 1(b).

In the heat-input simulation, voltages, representative of recovery temperatures, were switched in to cause current to flow through resistances, representative of the thermal resistance of the boundary layer, into various points of the resistance-capacitance network which represented the wing surface. Each of the voltages and resistances was adjusted to represent average values of the input functions for small time increments. In the present problem, the time span of the flight was divided into 20 equal increments of 10 seconds each. A ratio of analog time to flight time of 1 to 100 was used in the analog solutions.

Radiant heat losses from the surface are simulated by means of special resistors in which the current flow varies directly with the fourth power of the applied voltage, thus permitting an electrical representation of the radiant heat loss as set forth in equation (1). In all of the calculations performed on the analog in this investigation, the value of surface emissivity, ϵ, was taken as 0.8.

Recording System

To record the variations of voltage (which is analogous to temperature) with time occurring on the analog, a multichannel photographic oscillograph was used. Cathode followers, with high input impedances, were employed in the measuring circuits to avoid loading the analog circuit.

5

CONFIGURATIONS STUDIED

The study was concentrated on the leading-edge region of the wing. A view of the section of wing considered, showing the basic configuration studied, is given in figure 2. The skin back to the spar was divided into 15 segments for analysis on the analog. It was assumed that the leading-edge piece was attached to a wing afterbody. Internal heat transfer between inner surfaces of the wing was neglected.

The program was divided into three parts. The first encompassed a study of configurations with a 1/8-inch-thick Inconel-X skin with various filler materials in varying quantities located inside the leading-edge region to absorb the heat transferred at that point. Table I lists the configurations investigated.

The second part of the program consisted of a study of a skin composed of Inconel-X, 1/8-inch thick, with various conductive liners attached to the inner side of the skin in the leading-edge region to conduct heat away from the leading-edge point. These configurations are shown in table II. In all cases involving the internal addition of heat-absorbing material, the contact resistance between skin and heat absorber was taken as zero.

The third part was concerned with configurations consisting entirely of beryllium in the leading-edge region. Beryllium was selected for investigation because of its high specific heat and thermal conductivity, which were shown in reference 1 to be very desirable for heat-sink materials. Table III describes the configurations studied.

The thermal properties assumed for the various metals considered in the investigation are given in table IV. The values of thermal conductivity and specific heat were taken as constant, although they actually vary somewhat with temperature. The extent of the variation was not sufficient, however, to cause any large deviations in the results obtained.

FLIGHT TRAJECTORY ASSUMED FOR STUDY

The flight trajectory, as defined by Mach number, altitude, and angle of attack, is shown in figure 3. This boost-glide trajectory was used throughout the study.

Values of heat-transfer coefficient and recovery temperature were computed for the region near the leading edge by treatment of the forward portion as a swept circular cylinder. The calculations were performed by means of a method similar to that given in reference 6. Beyond the cylindrical portion, the wing was treated as a flat plate, with the

local properties of air being evaluated on the assumption of a gradual
Prandtl-Meyer expansion occurring downstream from the leading-edge
cylinder. Laminar flow was assumed for the entire leading-edge region.
Ideal-gas relationships were used throughout. The stagnation and leading-
edge points were taken as coincident for the entire trajectory. Standard-
atmosphere conditions were assumed for the properties of the ambient air.

To indicate the general order of magnitude of these calculated
values, the heat-transfer coefficient, stagnation temperature, and radia-
tion equilibrium temperature at the leading edge, for the two leading-
edge radii studied, are presented in figure 4.

RESULTS AND DISCUSSION

Leading-Edge Temperature Rise

The leading edge of a wing, being located at or near the aerodynamic
stagnation point, is subject to very high heating rates at supersonic
speeds. Because of the high rate of heating, this point usually is the
most critical from the standpoint of temperature rise. Broadly speaking,
the temperature rise of the leading-edge point under conditions of
transient aerodynamic heating can be restricted in two ways. The first
of these consists of locating materials with high thermal capacity behind
the leading edge to absorb the incoming heat, thereby creating sufficient
delay in the temperature rise to permit traversing the critical flight
regimes, when high heating rates occur, without allowing the surface
temperature to climb to excessively high values. The second method is to
provide sufficient conduction in the skin to draw the heat away from the
leading edge and distribute it in the cooler afterregions. Both of these
methods rely on absorption of the heat, which is governed by a combina-
tion of thermal capacitance (ρc_p) and thermal conductivity (k) of the
materials involved. In the following discussion, the relative merits of
each of the methods, and a combination of the two, will be considered.
The importance of capacity and conduction in limiting the leading-edge
temperature will also be discussed.

Inconel-X skin with various filler materials.- The influence of
varying the amount and type of filler material on the temperature rise
of the wing leading-edge point is shown in figure 5. A summary of the
temperature-rise data given in figure 5 is presented in figure 6, which
shows the depression in maximum temperature of the leading-edge point
achieved with the various filler materials as a function of the weight
of material. A study of this figure shows the weight of filler material
for a given temperature depression to be approximately inversely propor-
tional to the specific heat of the material, for the case of the larger
leading-edge radius, indicating a negligible influence of thermal con-
ductivity in reducing the leading-edge temperature. This result is
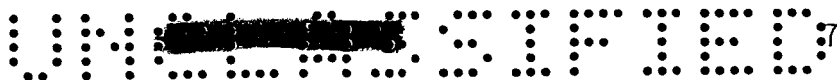
reasonable, since thermal capacity would be expected to govern the leading-edge temperature rise when the heat-absorbing material is concentrated in the leading-edge region.

As the leading-edge radius was reduced, the heat-flow path from the leading edge became more restricted, and the effect of thermal conductivity commenced to influence the temperature rise. This is illustrated in figure 6 by the data for a leading-edge radius of 0.188 inch. A comparison between the cases for the copper and beryllium filler materials shows the temperature depression still to be roughly inversely proportional to the specific heat; however, the increase in weight of copper filler was proportionately not as great as for beryllium, which has a lower conductivity.

The data of figure 6 indicate the advantage, from a weight standpoint, of utilizing a filler material of high specific heat, such as beryllium, in heat-sink applications. Consider, for example, the wing with a leading-edge radius of 0.47 inch. For a temperature depression of 600° R, the weight of beryllium filler required would be 0.4 pound per foot span, as contrasted with 2.0 pounds for Inconel-X and 2.5 pounds for copper.

Inconel-X skin with conductive liners.- Figure 7 shows the effect on the leading-edge temperature of adding a conductive internal liner to the skin in the leading-edge region. Several variations of the liner were studied to obtain an indication of the importance of conduction in reducing the leading-edge temperature.

Conduction is shown in figure 7 to provide a substantial reduction in leading-edge temperature. For example, the curves for configurations 24 and 25, which, in effect, represent configuration 1 with a greatly increased thermal conductance, but with no increase in thermal capacity, show that the maximum temperature was decreased by over 400° F by increasing the conduction. When the capacitance of the copper liner was included (configs. 22 and 23), the leading-edge temperature was reduced even further.

In view of the strong effect of conduction in removing heat from the leading edge, it is of interest to compare the effectiveness of a liner with that of a leading-edge filler in reducing the leading-edge temperature. Points representing copper liners 0.075 inch thick (config. 22) and 0.125 inch thick (config. 23) have been included in figure 6 to indicate the relative weight of liner material required for given temperature depressions. It is apparent from these data that, regardless of the beneficial influence of conduction in restricting the leading-edge temperature, the liner is not as efficient as the filler from a weight standpoint, and it is better to concentrate the heat-absorbing material back of the leading edge, rather than to spread the material out as a

liner, even for highly conductive metals. The effect of conduction on the temperature at the leading-edge point will be discussed further in a later section of this report.

Beryllium skin and filler material.- The leading-edge temperature-rise data for configurations consisting entirely of beryllium are given in figure 8. The temperature-rise data for the case of 1/8-inch-thick skin with no filler material show that changing the skin from Inconel-X (config. 1, fig. 5(a)) to beryllium (config. 27, fig. 8(a)) reduced the peak temperature from 2180° to 1820° R. Since the heat-absorbing capabilities of Inconel-X and beryllium are nearly equal for the same volume of metal, this 360° R reduction in temperature can be attributed almost entirely to the greater conductivity of beryllium, which permits the incoming heat to be conducted rapidly into the cooler regions.

The data of figure 8 have been summarized in figure 9, which presents the maximum temperature reached by the leading edge as a function of the weight of the leading-edge piece. The results for beryllium are compared in the figure with those for Inconel-X. The most obvious fact illustrated in figure 9 is the large saving in weight which could be achieved by substituting beryllium for Inconel-X. This is due primarily to the much greater specific heat of beryllium. The data of figure 9 also reveal that, because of the high conductivity of beryllium, the leading-edge temperature would not be greatly influenced by a decrease in leading-edge radius. Thus, through a reduction in the leading-edge radius, a reduction in the aerodynamic drag of the wing could be achieved, with only a very small weight penalty.

The outstanding virtues of beryllium as a heat-sink material can be illustrated by considering its advantages over Inconel-X for a typical wing leading-edge construction. For example, by changing the leading-edge material from Inconel-X to beryllium, it would be possible to reduce the maximum leading-edge temperature from 2200° to 1700° R, while reducing the weight of the leading-edge piece from 5 to 1-1/4 pounds per foot span, and at the same time reducing the wing drag by decreasing the leading-edge radius.[1]

The effect of increasing the skin thickness on the temperature-weight relationship for all-beryllium construction is shown in figure 9. These data show that, despite the increased conduction of heat from the leading edge, the resulting configurations were less efficient, requiring

---

[1]Although beryllium possesses favorable thermal properties, consideration must also be given to any unfavorable characteristics which might limit its use, such as brittleness, and susceptibility to oxidation when subjected to elevated temperatures for prolonged periods. At the present time, these limitations are not well established.

a greater weight of material for a given temperature limit than for the thinner skin. This further illustrates the desirability of providing proper distribution of the heat-absorbing material.

Influence of Conduction on Leading-Edge Temperature
for Skins of Uniform Thickness

In the past, it has been common practice to employ skins of uniform thickness in the leading-edge region of wings. Because of the simplicity of this type of construction, consideration no doubt will be given to its use in many future high-speed airplanes in which the leading-edge temperature must be controlled. Therefore, the data which have been taken for cases involving skins of uniform thickness will be analyzed briefly to illustrate the influence of conduction in removing heat and limiting the leading-edge temperature during transient heating.

Maximum temperature at leading edge.- The effect of a variation in the thermal conductivity of the skin on leading-edge temperature is shown in figure 10, which presents a plot of the maximum leading-edge temperature as a function of the conductivity of the skin. For this figure, the thermal capacity of the skin was constant, while the thermal conductivity was varied. The values were taken from the data for configurations 1, 24, 25, 26, and 27, which consisted of 1/8-inch-thick skin with different conductivities, but constant thermal capacitance.

Figure 10 shows the marked effect of increasing the thermal conductivity on the maximum temperature reached. As the conductivity was increased from 12.6 (Inconel-X) to 210 Btu/hr ft^2 $^\circ$F/ft (copper), the leading-edge temperature was decreased from 2180° to 1720° R, which represents a 26-percent decrease in temperature rise. The maximum possible decrease in temperature was 35 percent and is indicated in figure 10 by the line at 1550° R, which represents the maximum leading-edge temperature for the case of a perfectly conducting skin.

Heat flow at leading edge.- An analysis of the heat-flow rates at the leading edge provides further information on the importance of conduction in reducing the leading-edge temperature. Figure 11 compares curves of the calculated convective heat input to the leading-edge point with curves of the heat removed from the leading edge by conduction for skins of uniform thickness composed of Inconel-X (config. 1) and beryllium (config. 27). The conductive-loss curves were determined by subtracting the heat lost by radiation and that absorbed by the leading-edge skin from the calculated convective heat input.

Figure 11 reveals that a large percentage of the incoming heat to the leading edge was removed by conduction, even for the case of poorly conducting Inconel-X. For example, at 84 seconds, and again at 143 seconds, when the peaks occurred in the convective-input curve, the

conductive loss was about half the total heat input. When the skin
material was changed to beryllium, the conductive loss rose to about two-
thirds the convective input at the times of maximum heating. Thus, it is
evident that conduction can have a strong influence in alleviating the
adverse effects of high heating rates at wing leading edges.
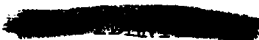

Surface-Temperature Distribution

Transient-temperature distributions.- Distributions of surface tem-
perature in the leading-edge region at 145 seconds, when the temperature
gradients were highest, are presented in figures 12, 13, and 14. These
figures show the distributions for the configurations considered in
figures 5, 7, and 8, respectively.

A review of the temperature-distribution curves shows that the most
uniform distributions were obtained with highly conductive filler materials
concentrated back of the leading edge (see, e.g., the distributions for
configurations 7 and 10, figs. 12(b) and (c)). The data for cases with
highly conductive skins but no filler, such as configuration 25, figure 13,
and configuration 30, figure 14(b), show fairly high temperature differ-
ences in the leading-edge region, in spite of the beneficial influence of
conduction. Thus, it is apparent that conduction alone cannot be relied
upon to promote uniform surface temperatures under conditions of transient
heating, and that concentration of the heat-absorbing material in the
regions of high heating rate is important from the standpoint of uniform
temperature distribution.

Reduction in the leading-edge radius increased the temperature
gradients near the leading edge for configurations with Inconel-X skins
(figs. 12(e) and (f)). When the skin material was changed to beryllium,
for the case of the reduced leading-edge radius, the local temperature
gradients were greatly reduced, because of the higher conductivity
(fig. 14(c)). The resulting thermal gradients for the all-beryllium
cases with reduced leading-edge radius were, in fact, less than those
which existed for all-Inconel-X construction with a larger leading-edge
radius (fig. 12(a)). This emphasizes the desirability of employing
materials of high conductivity, as well as high specific heat, in
leading-edge heat-sink applications.

Steady-state temperature distributions.- Temperature distributions
were obtained under steady-state conditions for several configurations in
order to illustrate the differences in distribution obtained between
transient and steady-state conditions. The data were obtained for the
conditions at 140 seconds, when the Mach number was 6.15 and the altitude
119,000 feet. The temperature distributions are shown in figure 15.

It is apparent from figure 15 that the advantages shown under
transient-heating conditions for configuration 7 (see fig. 12(b)), with

the filler material concentrated in the leading edge, no longer prevailed under steady-state conditions. Instead, the configuration possessing high conductivity in the skin (config. 23) produced a more uniform temperature distribution. The line for configuration 26, with perfect conduction, represents the minimum temperature to which the leading edge could be reduced.

CONCLUSIONS

A study of the influence of internal modifications to a wing leading-edge region on the temperature rise and distribution under conditions of transient aerodynamic heating has led to the following conclusions:

1. For configurations with heat-sink material concentrated in the leading-edge region, the relative weight of material required to limit the leading-edge temperature to a given value is approximately inversely proportional to the specific heat of the material when the leading-edge radius is large. In this case, thermal conductivity has very little effect on the leading-edge temperature. When the leading-edge radius is small, thermal conductivity, as well as specific heat, becomes important in influencing temperature rise and temperature distribution.

2. Thermal conductivity plays a major role in limiting leading-edge temperature when the skin is uniform in thickness. Under certain conditions, conduction can remove two-thirds or more of the incoming heat to the leading edge.

3. Because of the high specific heat and thermal conductivity of beryllium, this metal appears very attractive as a heat-sink material. In a comparison with Inconel-X, it was shown that by substituting beryllium, the maximum leading-edge temperature would be reduced, a severalfold saving in weight would be achieved, the aerodynamic drag of the wing could be reduced through a decrease in leading-edge radius, and the resulting temperature distribution would be more uniform.

Ames Aeronautical Laboratory
        National Advisory Committee for Aeronautics
                Moffett Field, Calif., Nov. 21, 1957

REFERENCES

1. Stalder, Jackson R.: The Useful Heat Capacity of Several Materials for Ballistic Nose-Cone Construction. NACA TN 4141, 1957.

2. Paschkis, Victor, and Baker, H. D.: A Method for Determining
    Unsteady-State Heat Transfer by Means of an Electrical Analogy.
    Trans. A.S.M.E., vol. 64, no. 2, Feb. 1942, pp. 105-112.

3. Avrami, M., and Paschkis, V.: Application of an Electric Model to
    the Study of Two-Dimensional Heat Flow. Trans. American Inst. of
    Chem. Engrs., vol. 38, no. 3, June 25, 1942, pp. 631-652.

4. Bromberg, R., and Martin, W.: Theory and Development of a Thermal
    Analyzer. (Final rep.) Dept. of Engr., UCLA, Aug. 1947.

5. Neel, Carr B.: A Procedure for the Design of Air-Heated Ice-
    Prevention Systems. (Appendix B) NACA TN 3130, 1954.

6. Reshotko, Eli, and Beckwith, Ivan E.: Compressible Laminar Boundary
    Layer Over a Yawed Infinite Cylinder With Heat Transfer and
    Arbitrary Prandtl Number. NACA TN 3986, 1957.

TABLE I.- CONFIGURATIONS WITH INCONEL-X SKIN AND VARIOUS
HEAT-ABSORBING MATERIALS BACK OF LEADING EDGE
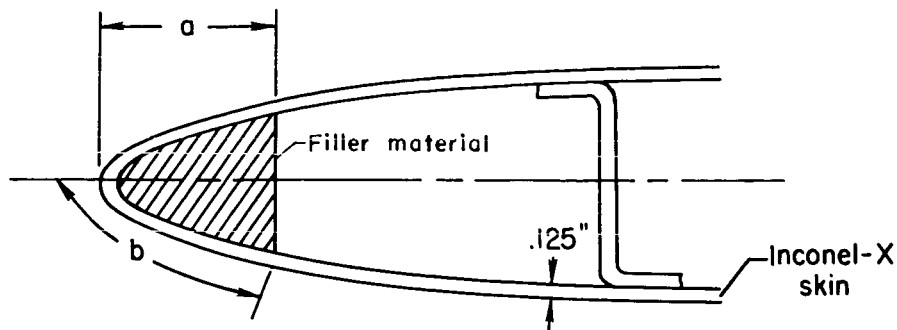
Configuration number	Filler material	Dimension a, in.	Dimension b, in.	Weight of filler, lb/ft span	Data figure numbers
(a) Leading-edge radius = 0.47 in.					
1	None	0.125	0	0	5(a),12(a)
a2	Inconel-X	.25	.65	.21	5(a),12(a)
3	Inconel-X	.47	.65	.84	5(a),12(a)
4	Inconel-X	.82	1.00	2.12	5(a),12(a)
5	Copper	.47	.65	.91	5(b),12(b)
6	Copper	.82	1.00	2.28	5(b),12(b)
7	Copper	1.17	1.35	4.25	5(b),12(b)
8	Aluminum	.82	1.00	.69	5(c),12(c)
9	Aluminum	1.17	1.35	1.16	5(c),12(c)
10	Aluminum	1.52	1.70	1.66	5(c),12(c)
11	Beryllium	.47	.65	.19	5(d),12(d)
12	Beryllium	.82	1.00	.46	5(d),12(d)
13	Beryllium	1.17	1.35	.86	5(d),12(d)
(b) Leading-edge radius = 0.188 in.					
14	None	.125	0	0	5(e),12(e)
15	Copper	.54	.61	.46	5(e),12(e)
16	Copper	.89	.96	1.22	5(e),12(e)
17	Copper	1.21	1.31	2.27	5(e),12(e)
18	Copper	1.56	1.66	3.57	5(e),12(e)
19	Beryllium	.89	.96	.25	5(f),12(f)
20	Beryllium	1.21	1.31	.46	5(f),12(f)
21	Beryllium	1.56	1.66	.72	5(f),12(f)

aSee figure 5(a) for details of filler geometry.

TABLE II.- CONFIGURATIONS WITH INCONEL-X SKIN AND CONDUCTIVE LINERS
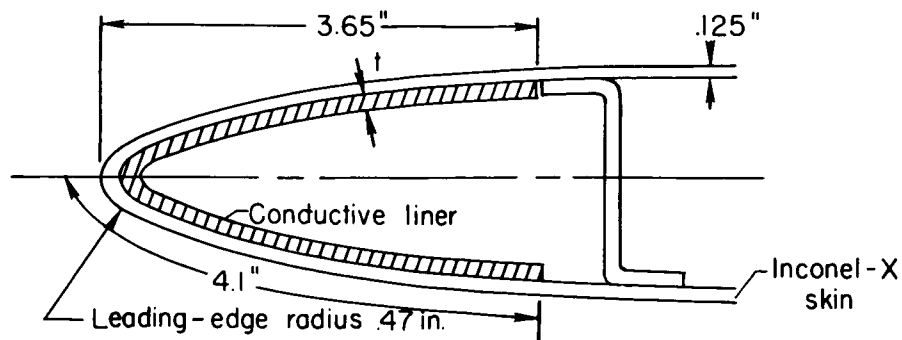
Configuration number	Liner material	Liner thickness, t, in.	Thermal conductivity of liner, Btu/hr ft² °F/ft	Specific heat of liner, Btu/lb °F	Weight of liner, lb/ft span	Data figure numbers
22	Copper	0.075	210	0.10	2.86	7,13
23	Copper	.125	210	.10	4.72	7,13
24	Copper	.075	210	0	0	7,13
25	Copper	.125	210	0	0	7,13
26	Perfectly conducting		∞	0	0	7,13

TABLE III.- CONFIGURATIONS WITH LEADING-EDGE PIECE COMPOSED
ENTIRELY OF BERYLLIUM

Extent of leading-edge piece
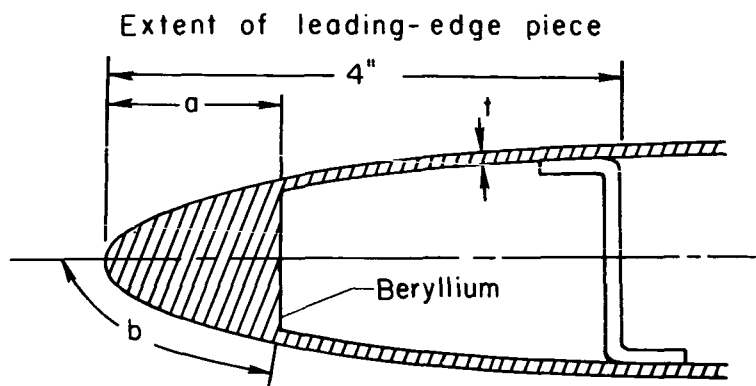
Configu-ration number	Skin thickness, t, in.	Dimension a, in.	Dimension b, in.	Weight of leading-edge piece, lb/ft span	Data figure numbers
(a) Leading-edge radius = 0.47 in.					
27	0.125	0.125	0	1.09	8(a),14(a)
28	.125	.47	.65	1.26	8(a),14(a)
29	.125	.82	1.00	1.54	8(a),14(a)
30	.188	.188	0	1.62	8(b),14(b)
31	.188	.47	.65	1.72	8(b),14(b)
32	.188	.82	1.00	1.97	8(b),14(b)
(b) Leading-edge radius = 0.188 in.					
33	.125	.125	0	1.06	8(c),14(c)
34	.125	.54	.61	1.10	8(c),14(c)
35	.125	.89	.96	1.25	8(c),14(c)
36	.188	.188	0	1.62	8(d),14(d)
37	.188	.54	.61	1.64	8(d),14(d)
38	.188	.89	.96	1.71	8(d),14(d)

TABLE IV.- PROPERTIES OF MATERIALS CONSIDERED IN STUDY
OF LEADING-EDGE HEATING

Material	Thermal conductivity, Btu/hr ft^2 ^{o}F/ft	Specific heat, Btu/lb ^{o}F	Density, lb/in.^{3}	Melting temperature, ^{o}R
Aluminum	130	0.22	0.0978	1680
Beryllium	93	.63	.0658	2800
Copper	210	.10	.322	2440
Inconel-X	12.6	.13	.300	3030
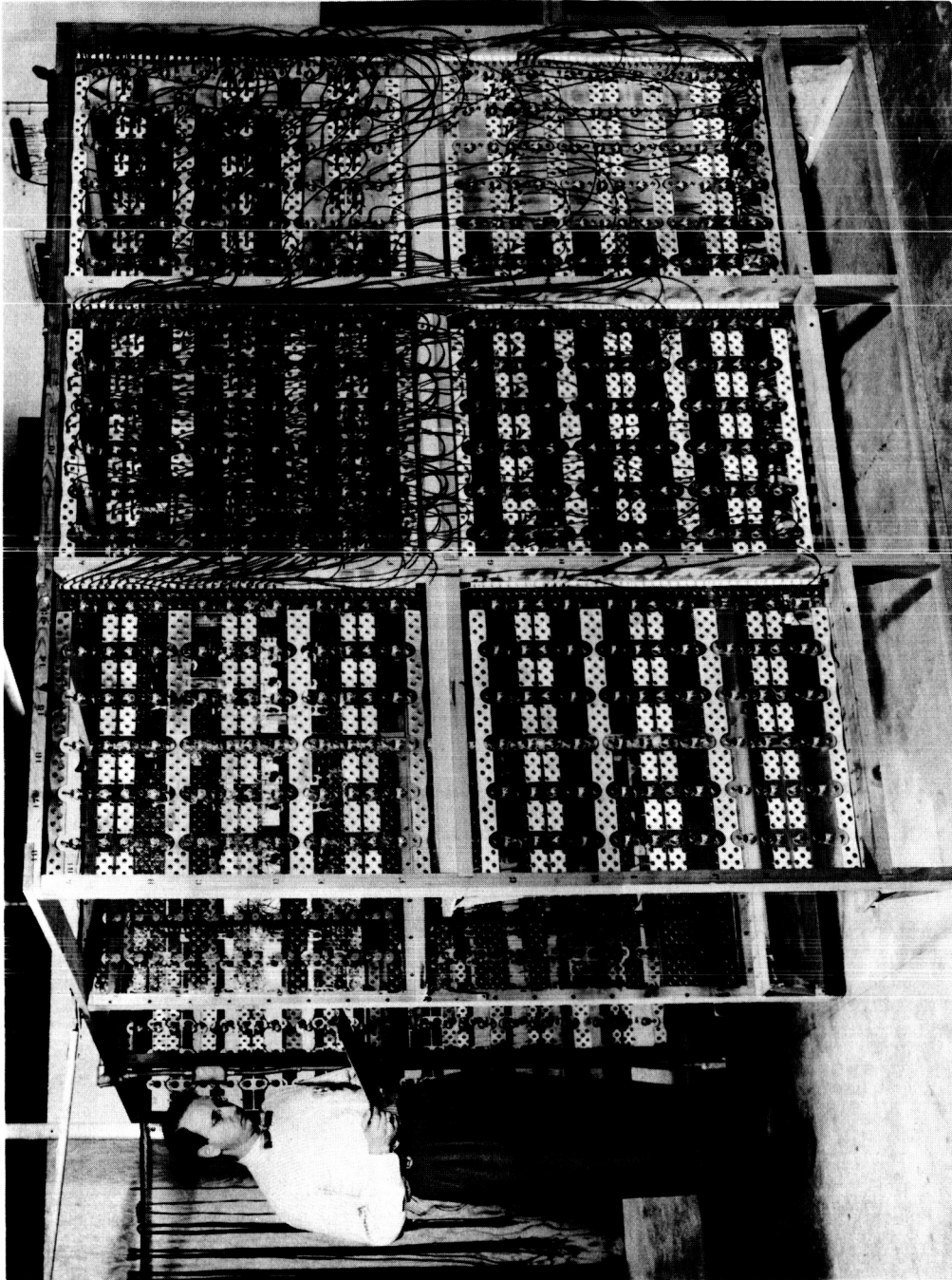
A-20368

(a) Resistance-capacitance network for simulating thermal circuit of body.

Figure 1.- Electrical heat-flow analog used in study of wing leading-edge heating.
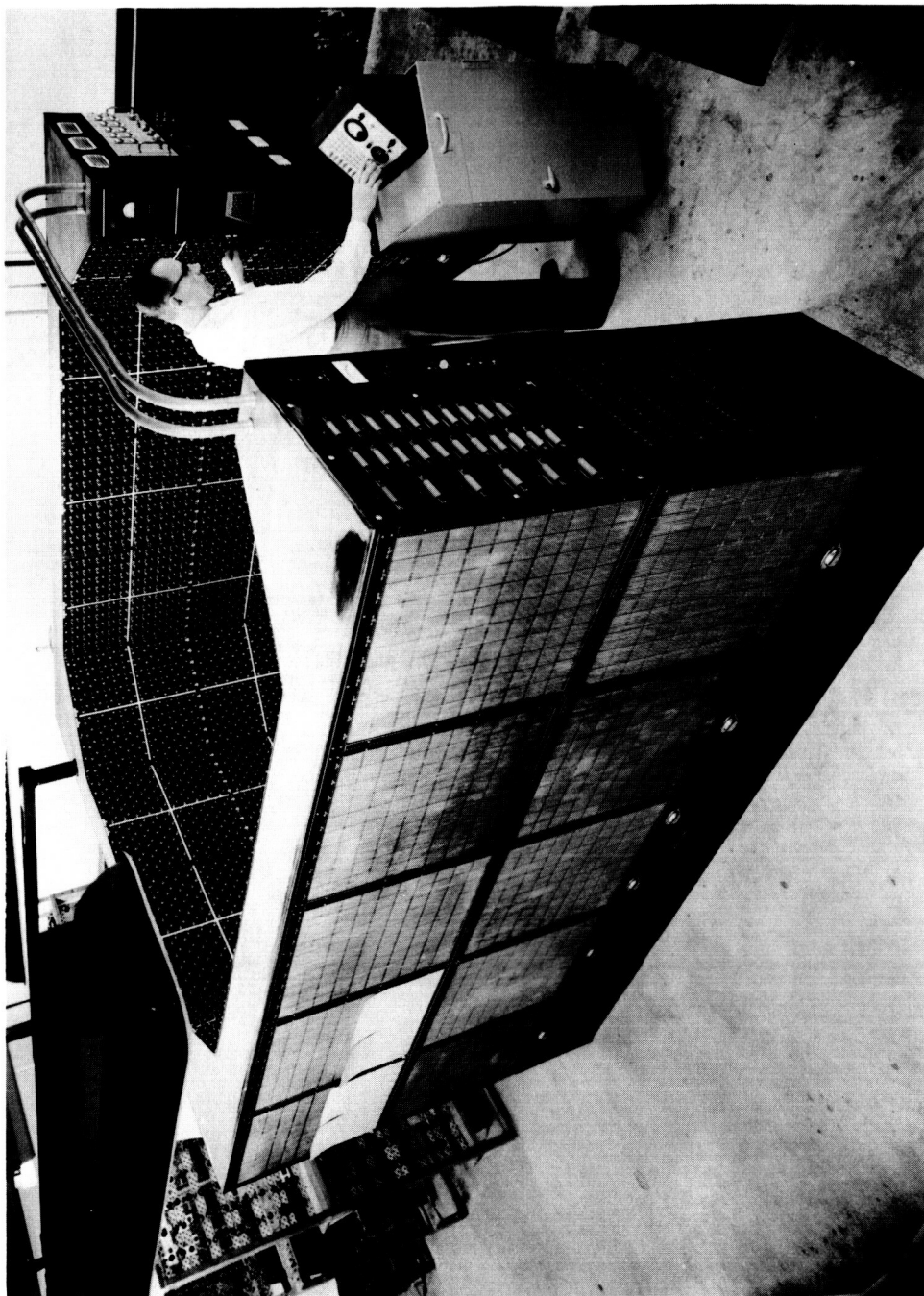
A-22560

(b) Input-function-generating equipment for simulating external heating conditions.

Figure 1.- Concluded.

←37° sweep angle

Air-stream
direction

Wing leading
edge

A

A

PLAN VIEW

4"

1.8"

VIEW A-A
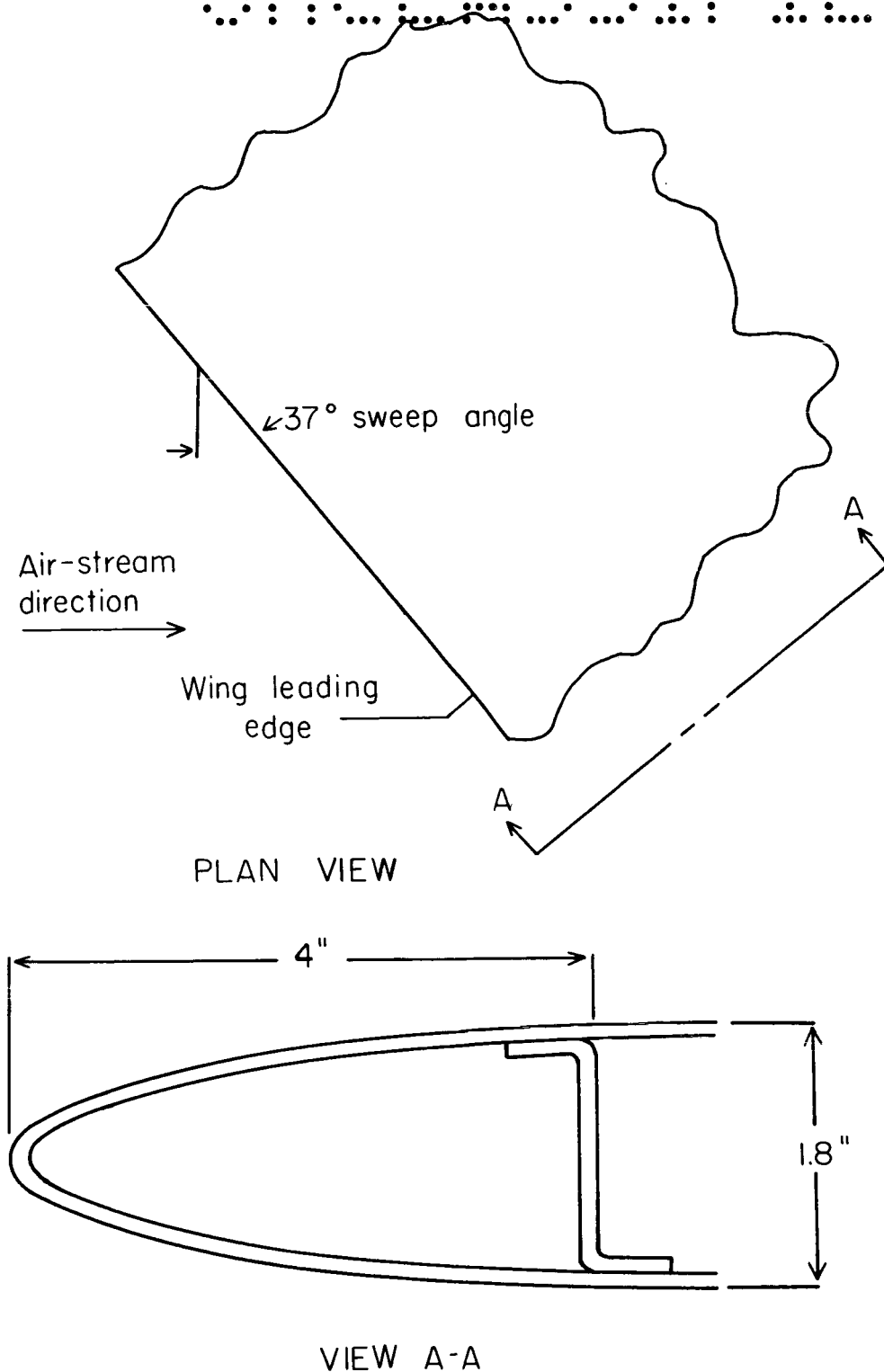
Figure 2.- View of segment of wing studied.
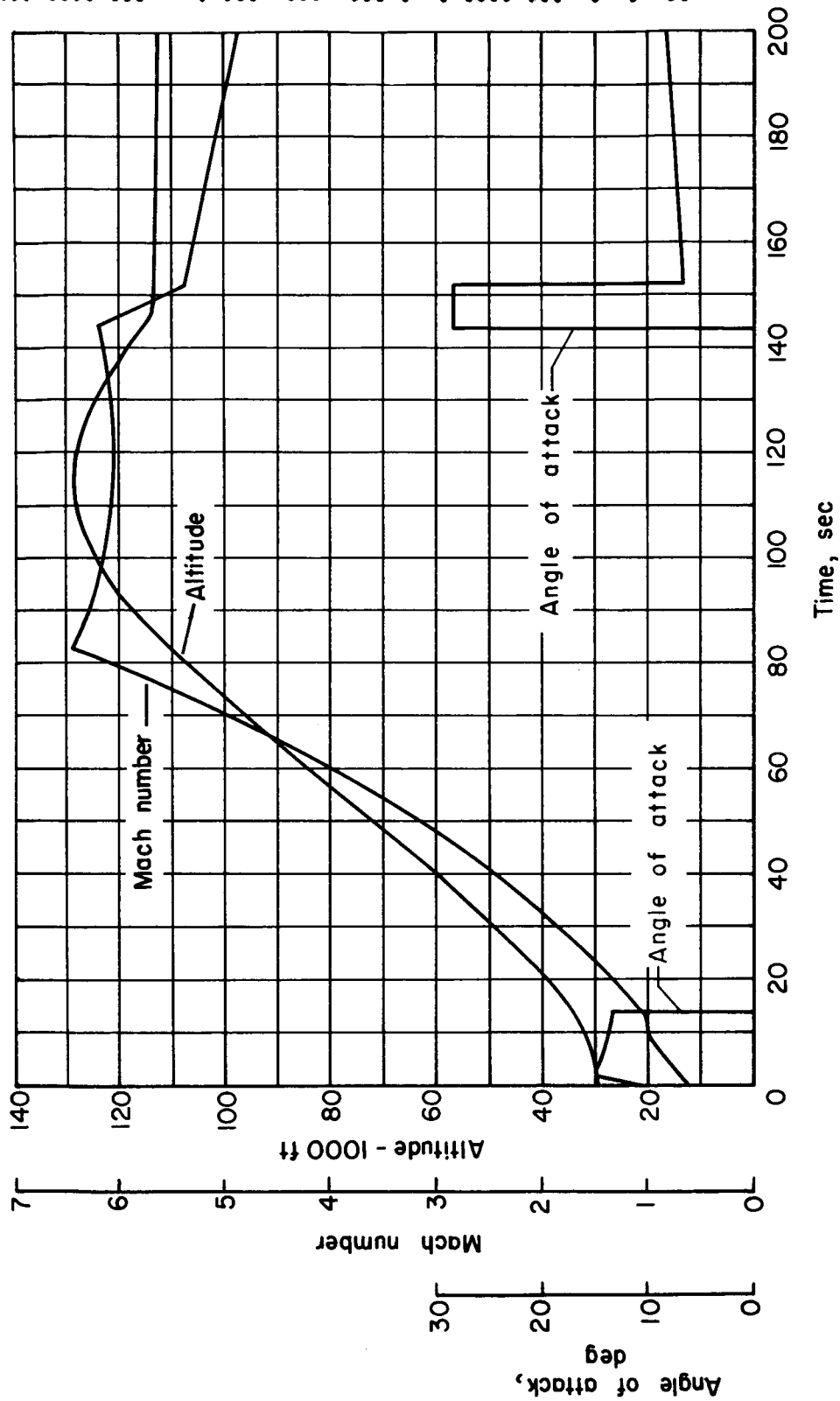
Figure 3.- Flight conditions assumed for study of wing leading-edge heating.

UNCLASSIFIED
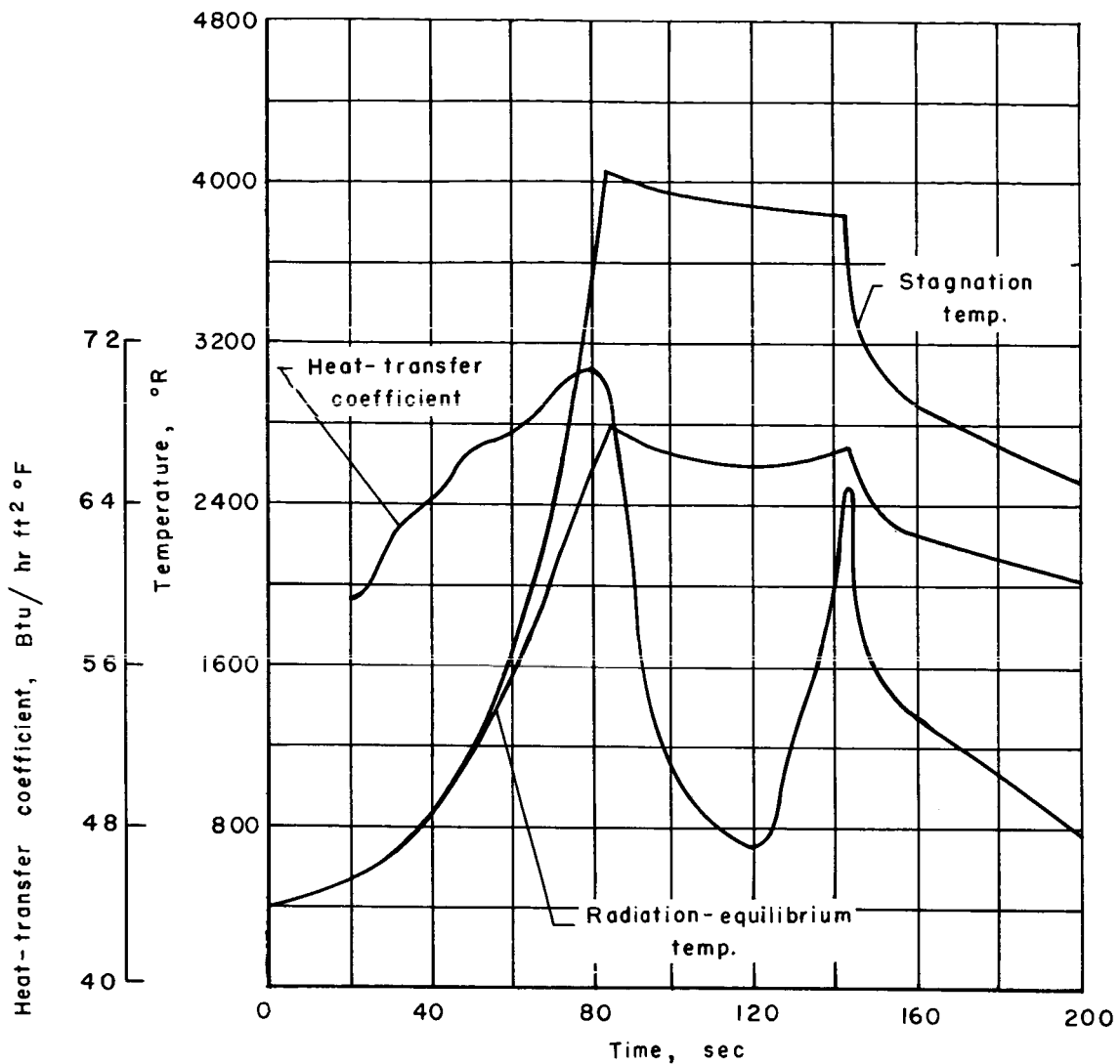
(a) Leading-edge radius = 0.47 in.

Figure 4.- Calculated heat-transfer coefficient, stagnation temperature, and radiation equilibrium temperature at wing leading edge.
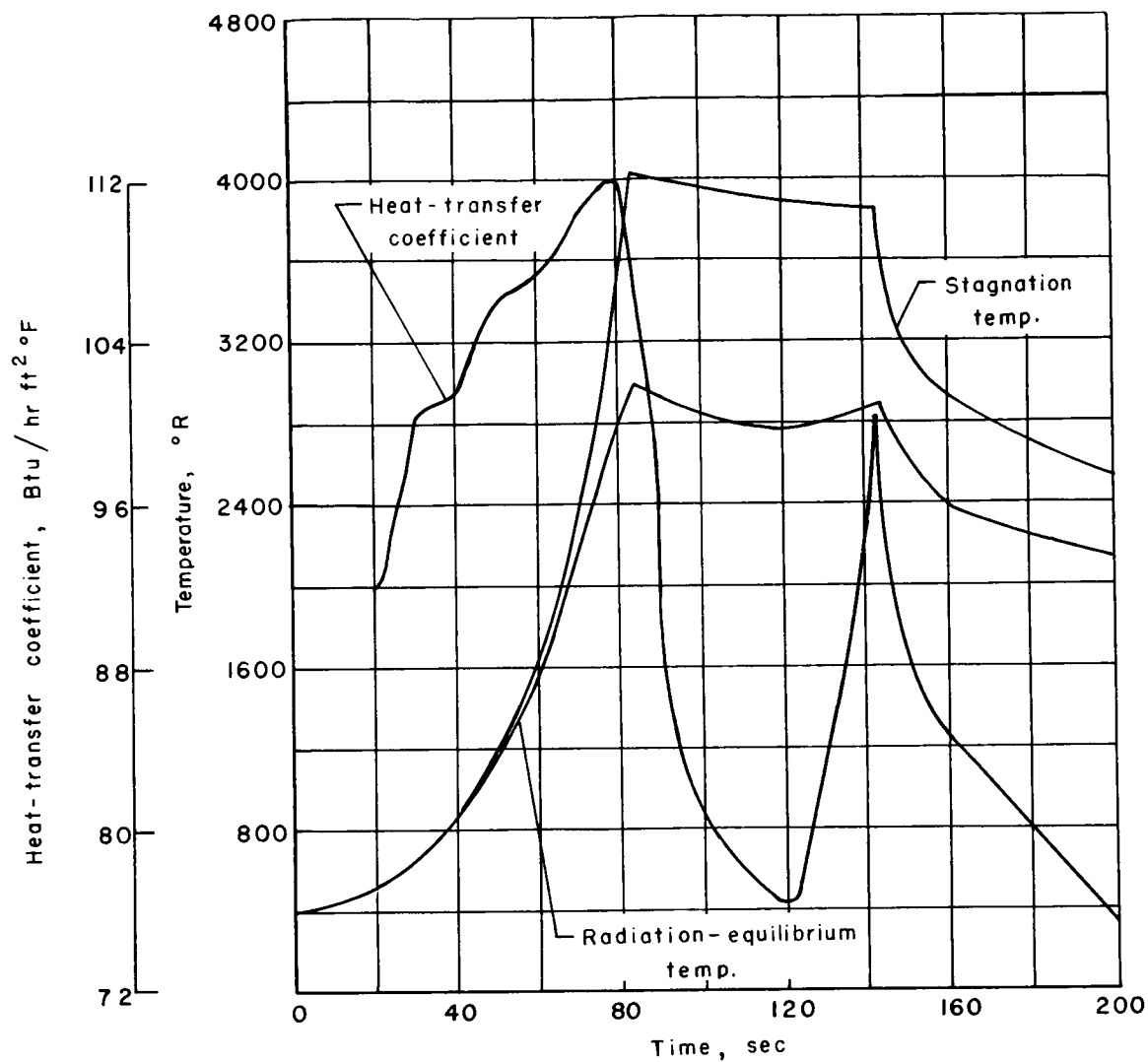
(b) Leading-edge radius = 0.188 in.

Figure 4.- Concluded.
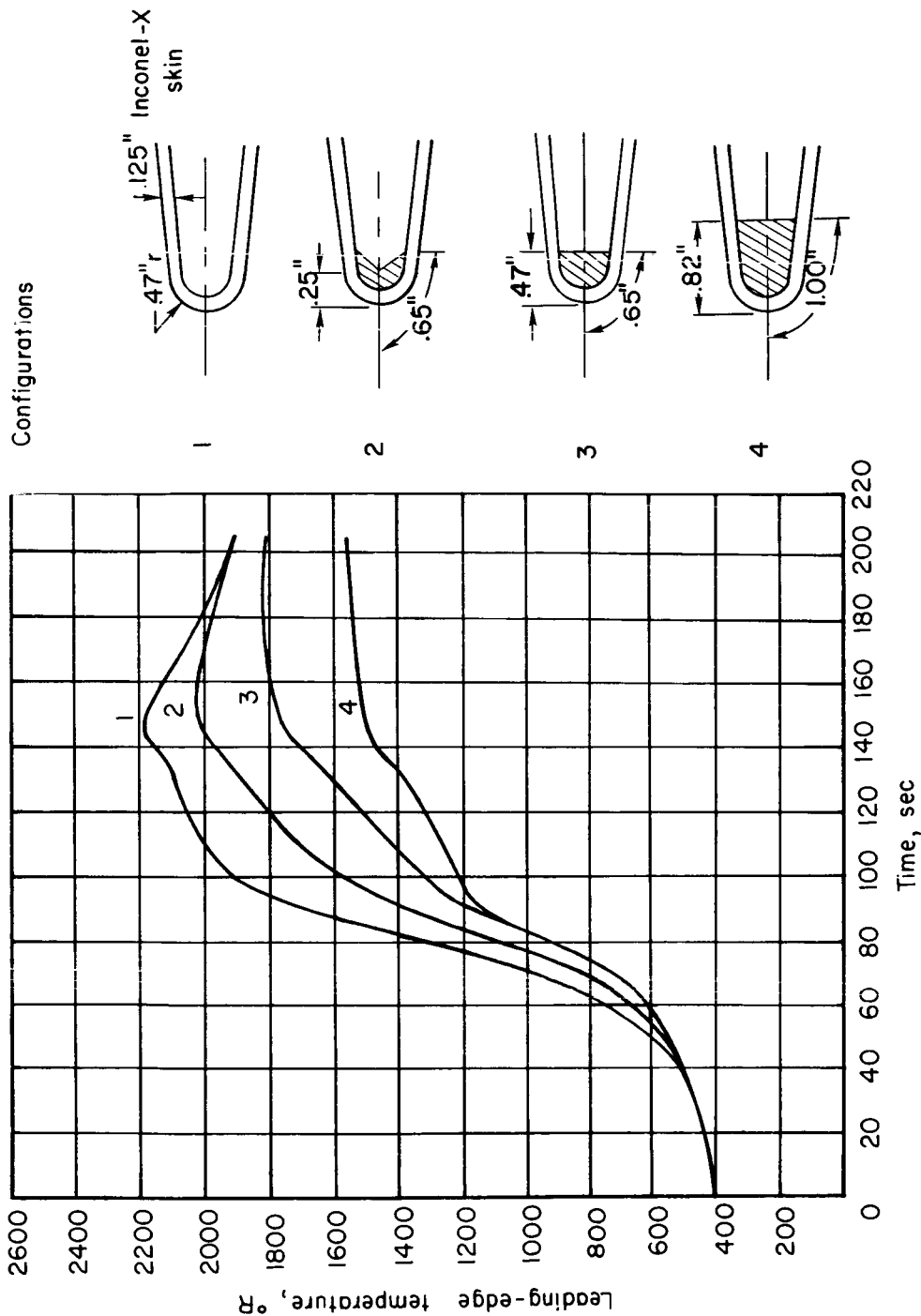
(a) Inconel-X filler material; leading-edge radius = 0.47 in.

Figure 5.- Variation of leading-edge temperature with time for various amounts of heat-absorbing material concentrated at leading edge.
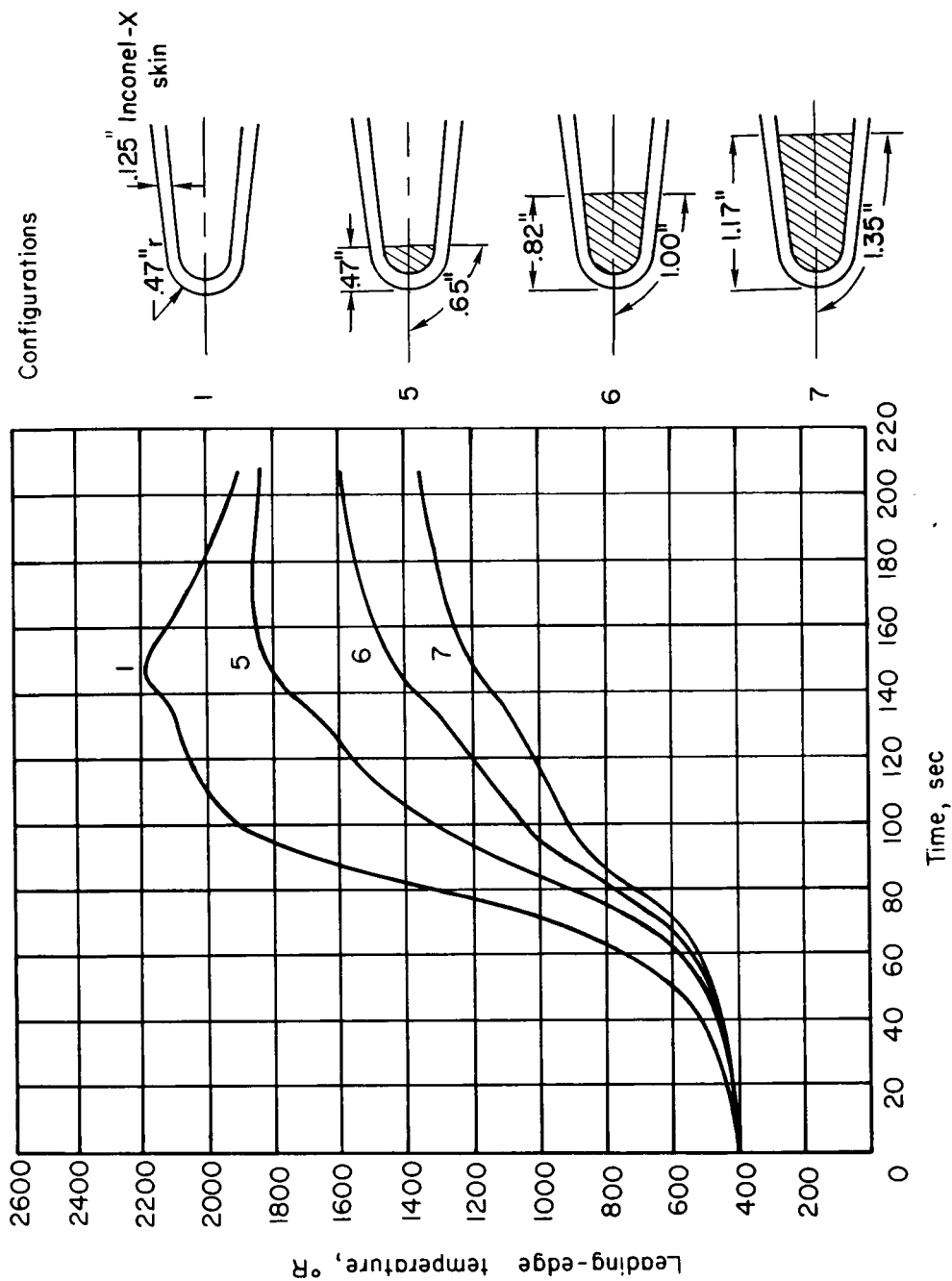
(b) Copper filler material; leading-edge radius = 0.47 in.
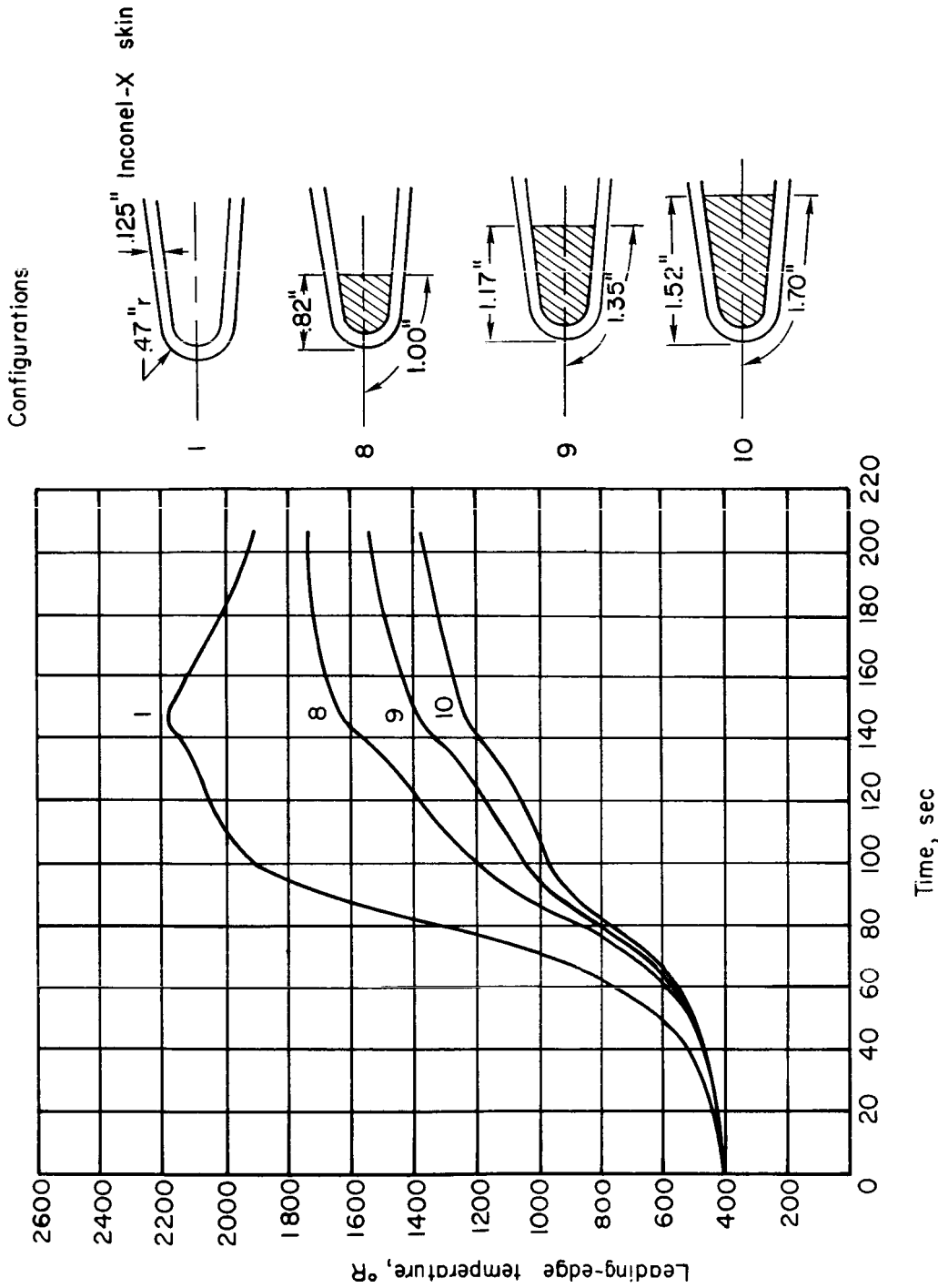
Figure 5.- Continued.

(c) Aluminum filler material; leading-edge radius = 0.47 in.
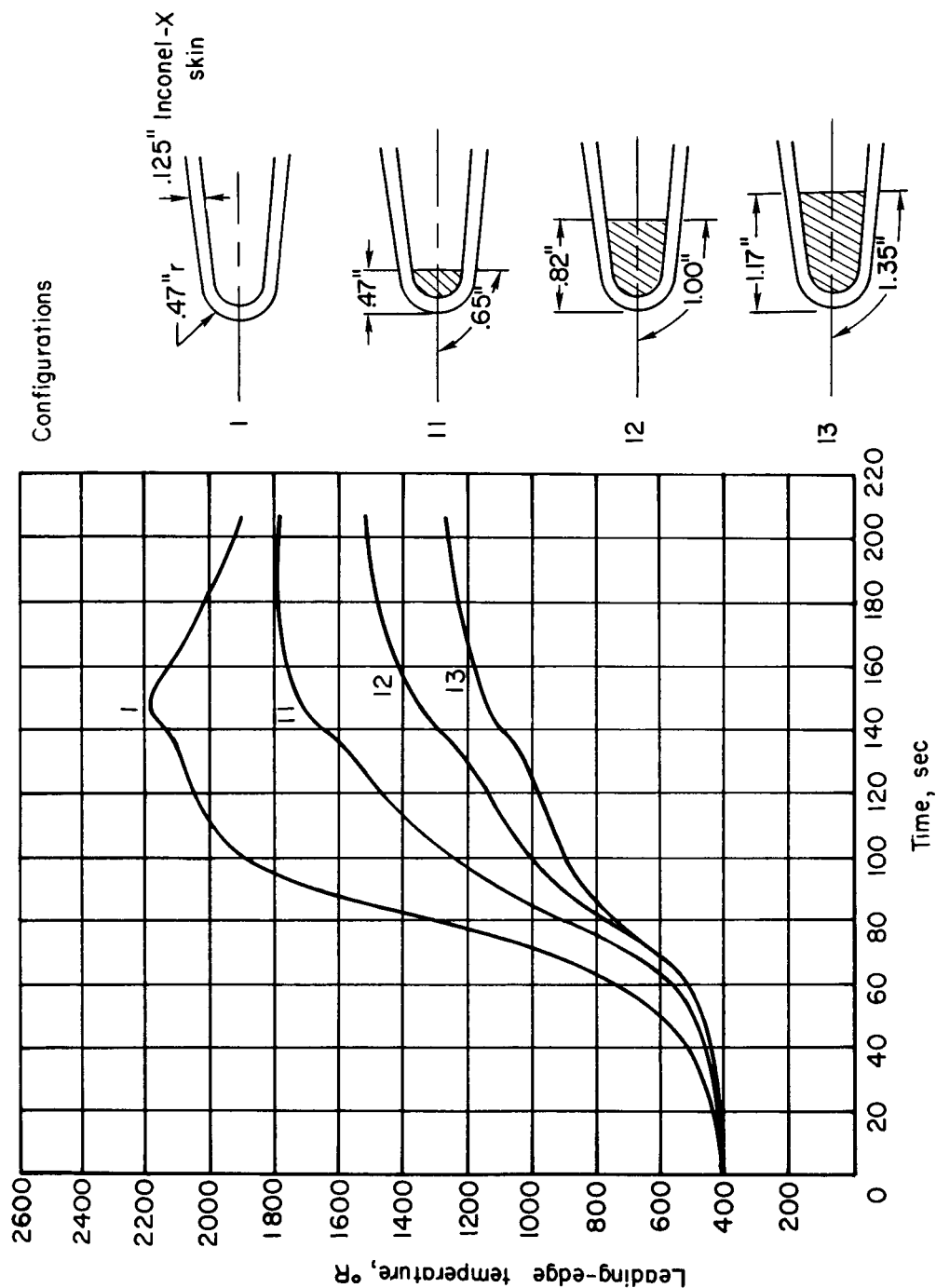
Figure 5.- Continued.

Configurations

.125" Inconel-X skin

.47" r

.47"   .65"

.82"   1.00"

1.17"   1.35"

(d) Beryllium filler material; leading-edge radius = 0.47 in.
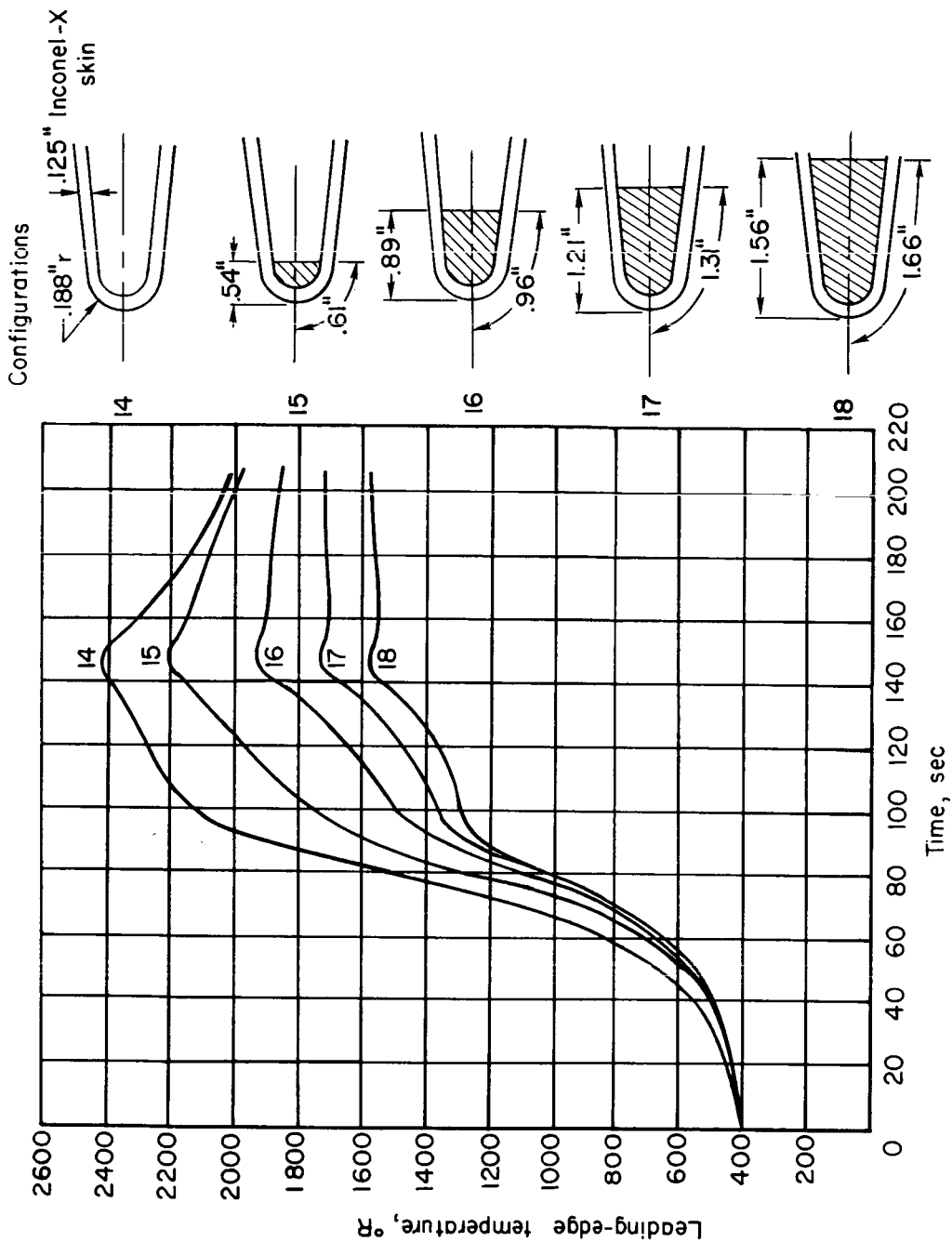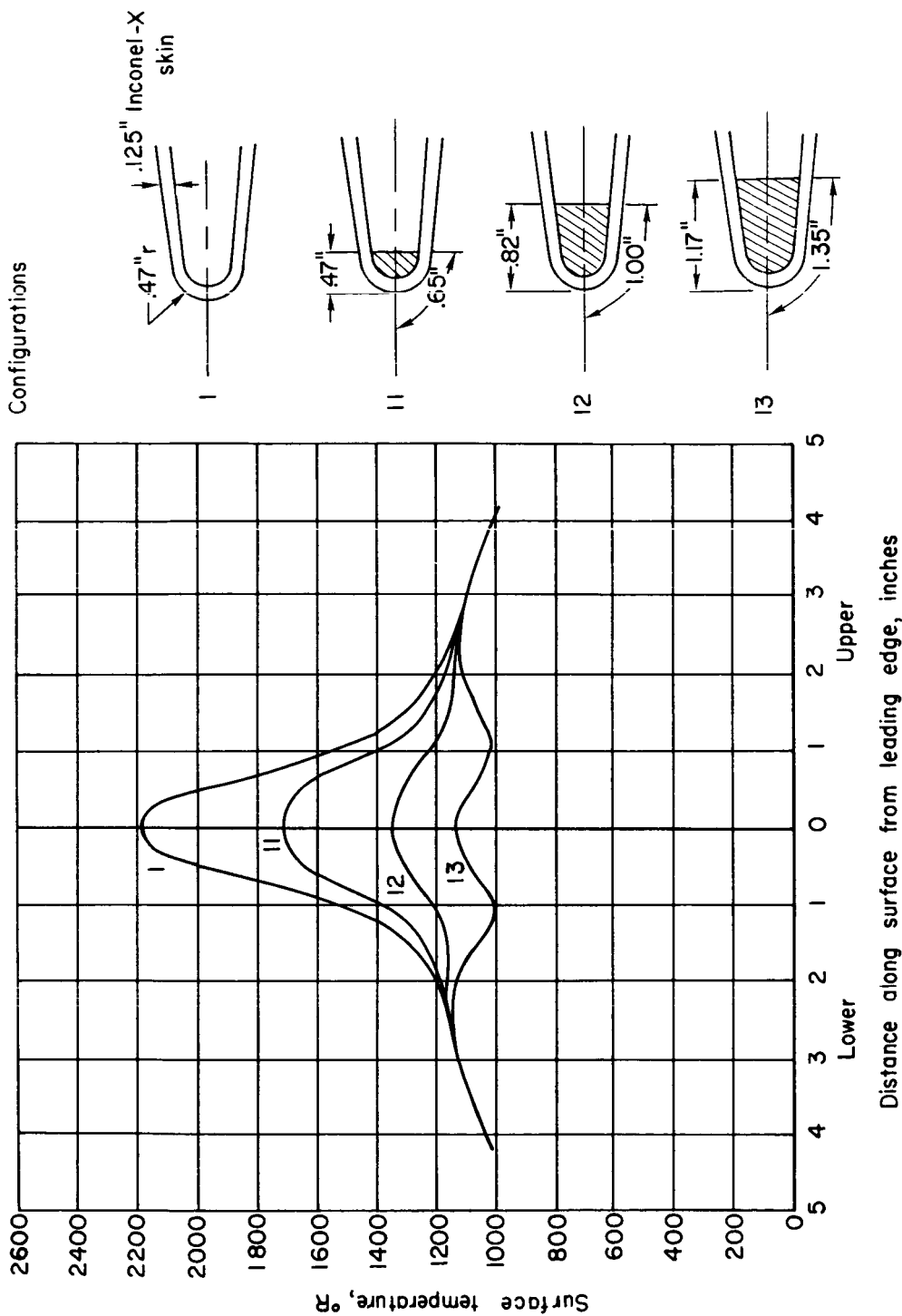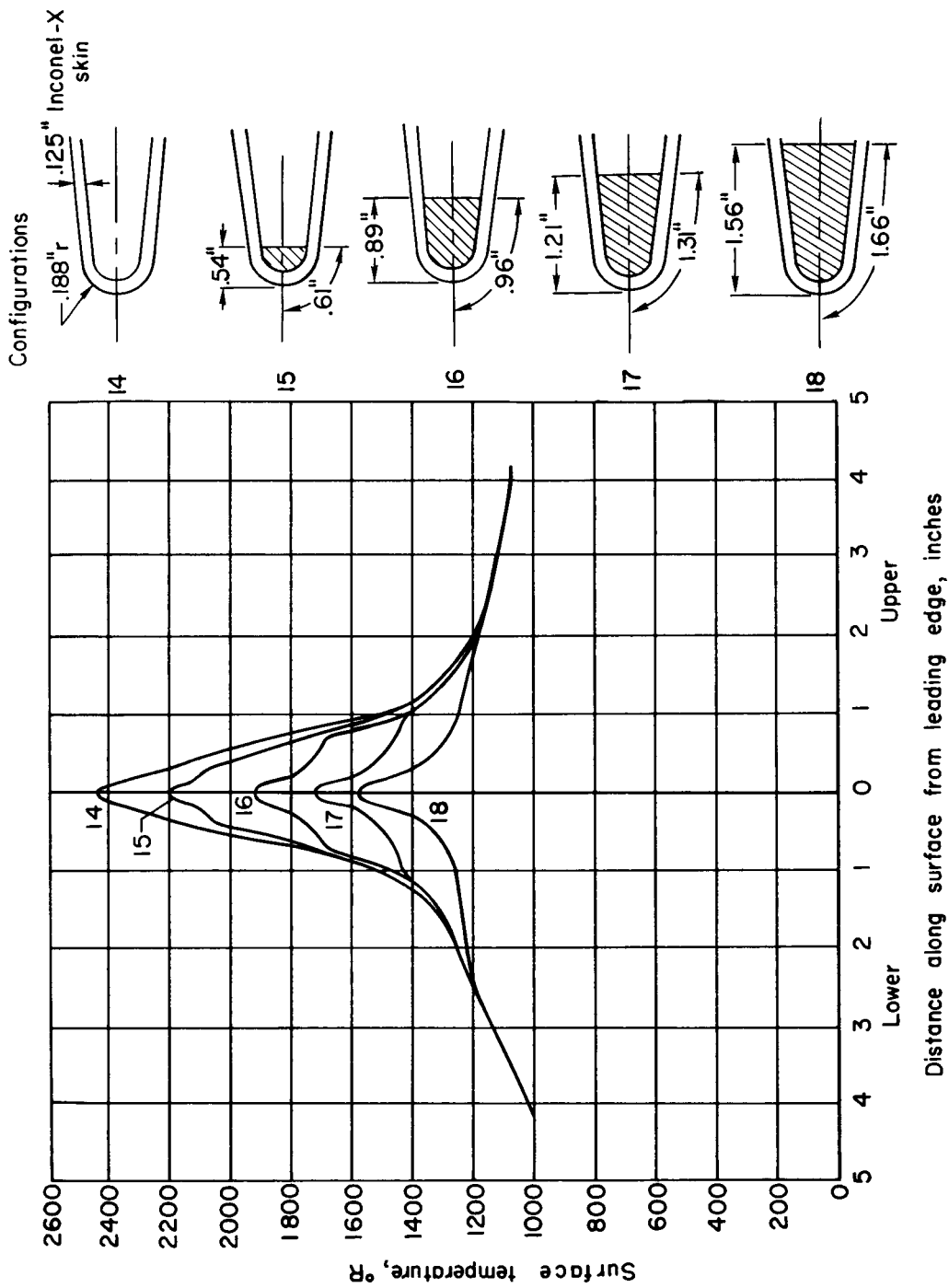
Figure 5.- Continued.

(e) Copper filler material; leading-edge radius = 0.188 in.

Figure 5.- Continued.
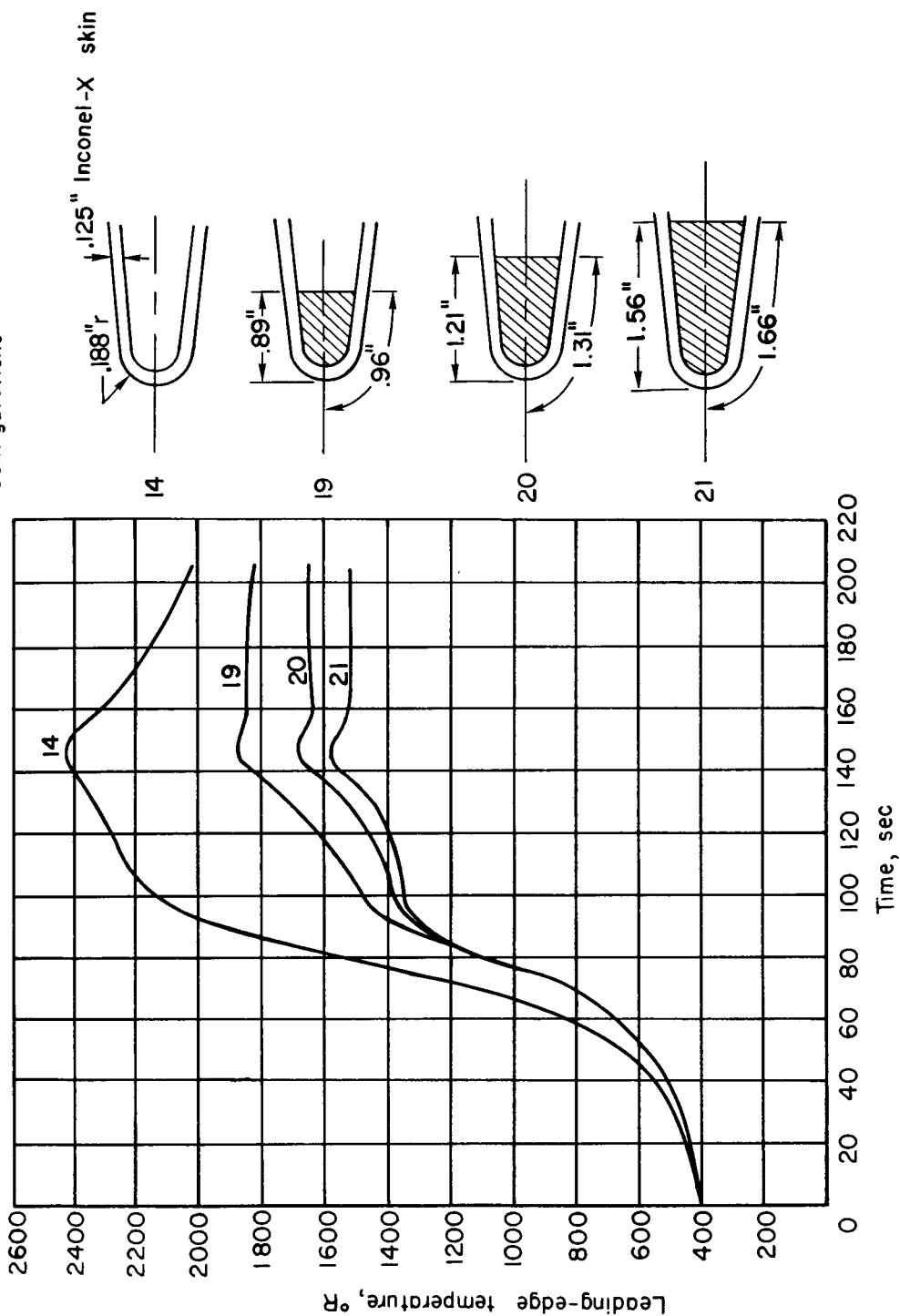
(f) Beryllium filler material; leading-edge radius = 0.188 in.

Figure 5.- Concluded.
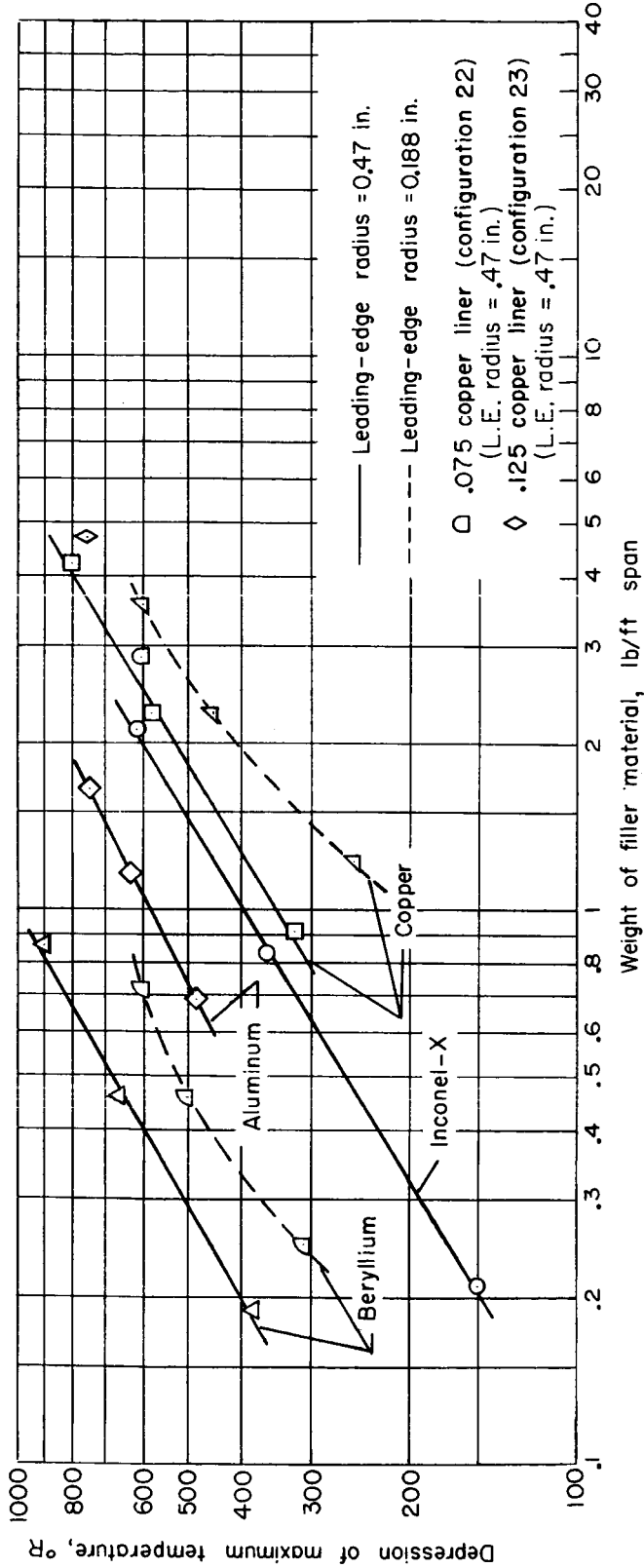
Figure 6.- Influence of internal addition of metal at wing leading edge on depression of maximum temperature.
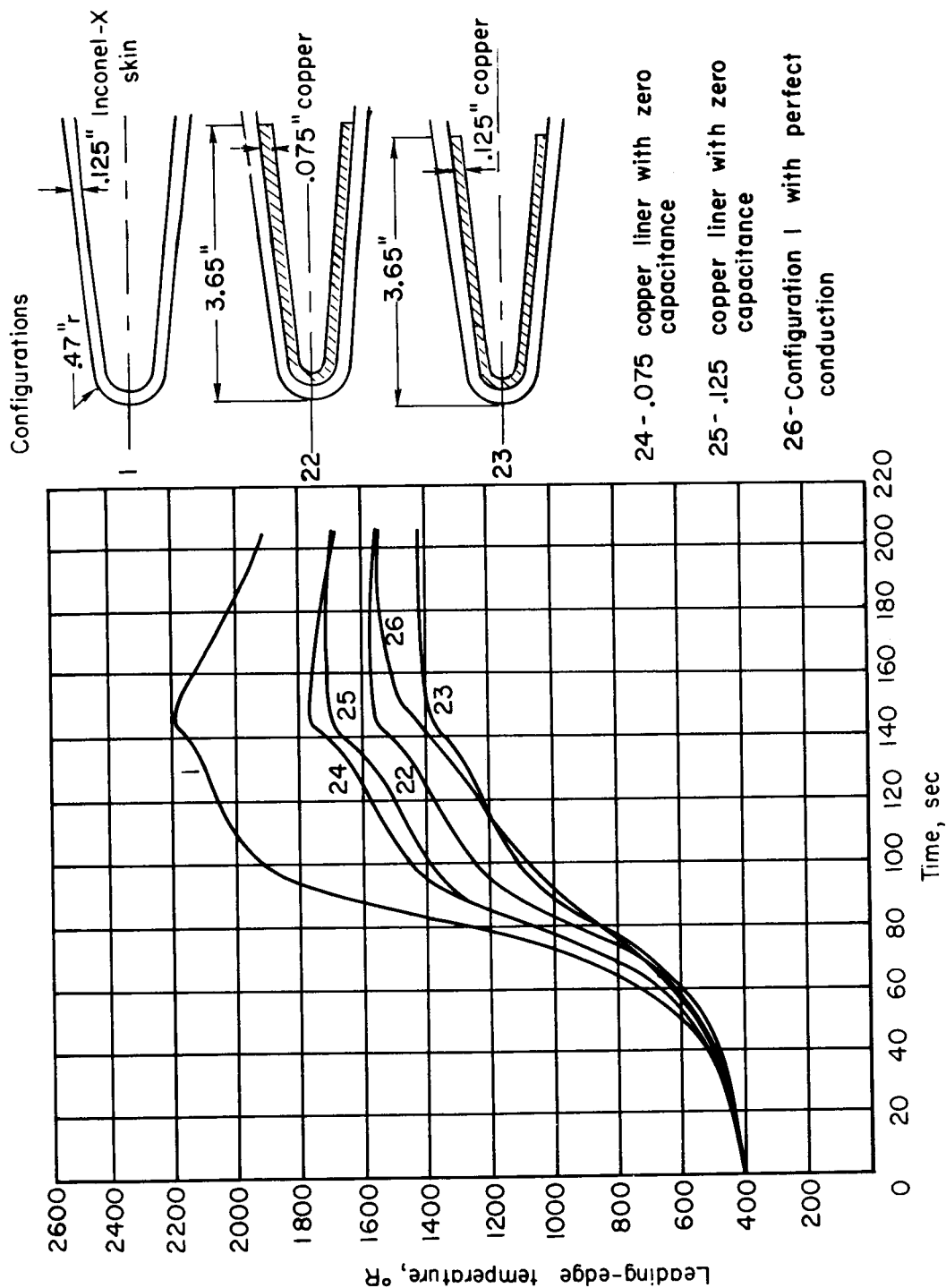
Figure 7.— Variation of leading-edge temperature with time for various arrangements of heat-conducting material distributed uniformly around interior of leading-edge region.
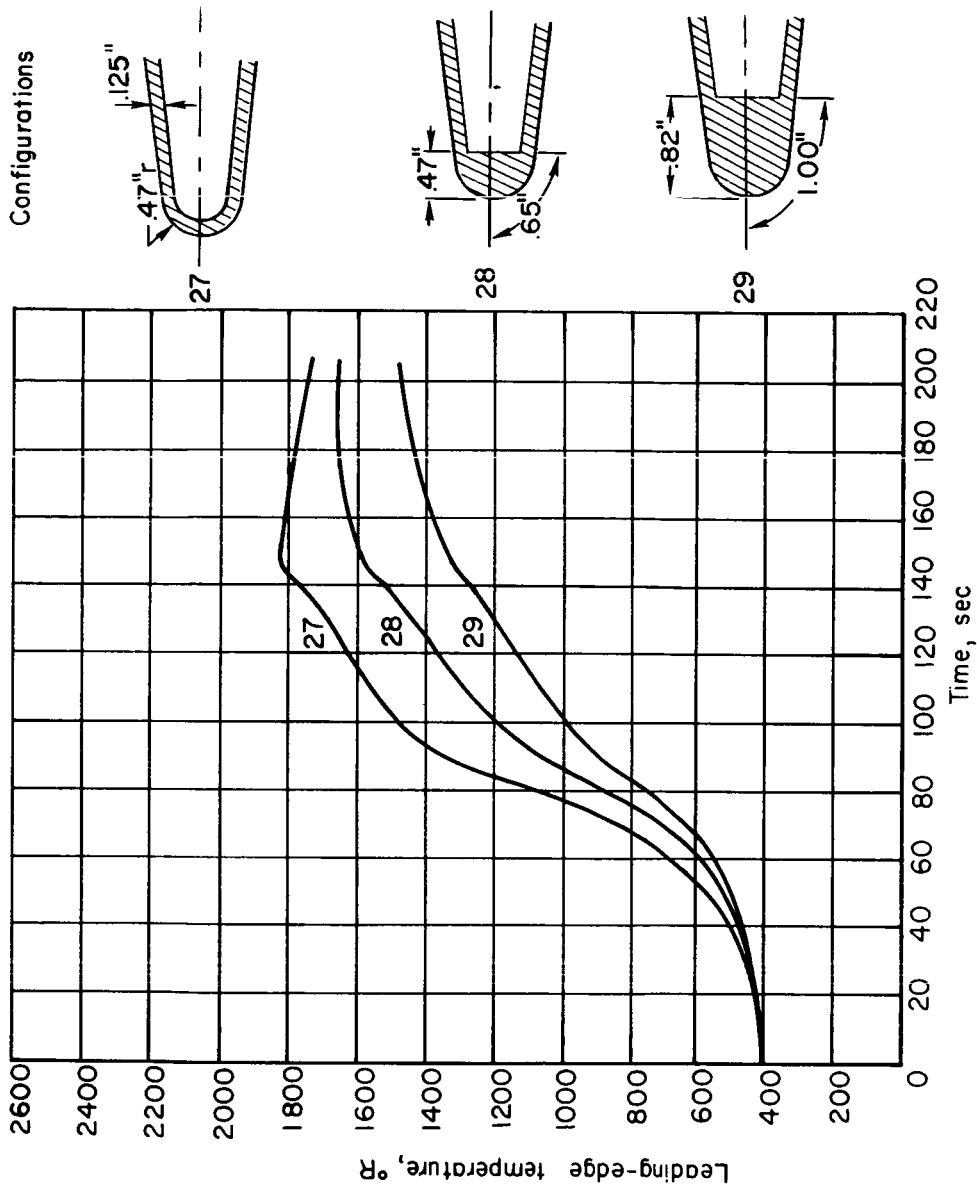
(a) Leading-edge radius = 0.47 in.; skin thickness = 0.125 in.

Figure 8.- Variation of leading-edge temperature with time for various configurations composed entirely of beryllium.
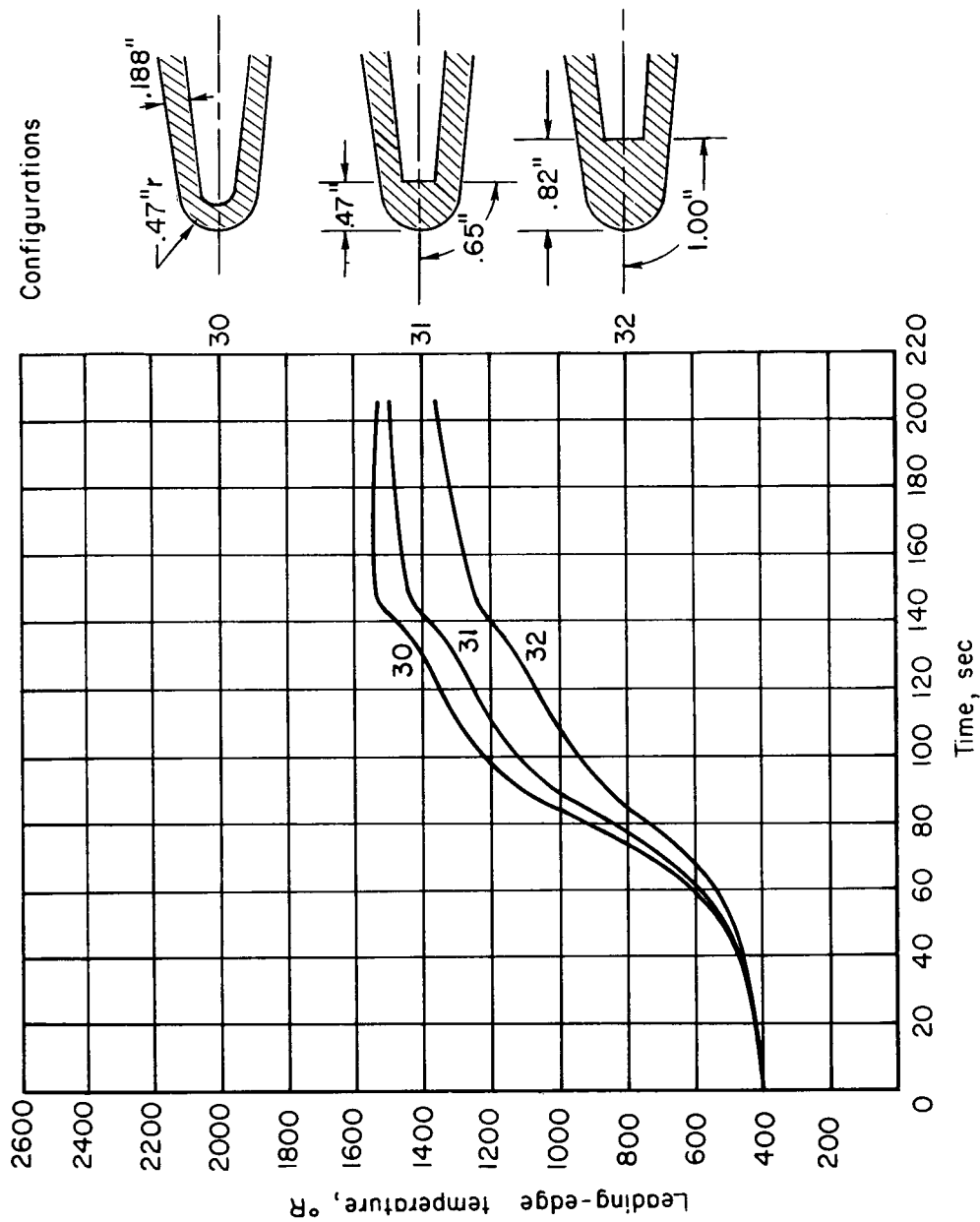
(b) Leading-edge radius = 0.47 in.; skin thickness = 0.188 in.

Figure 8.- Continued.
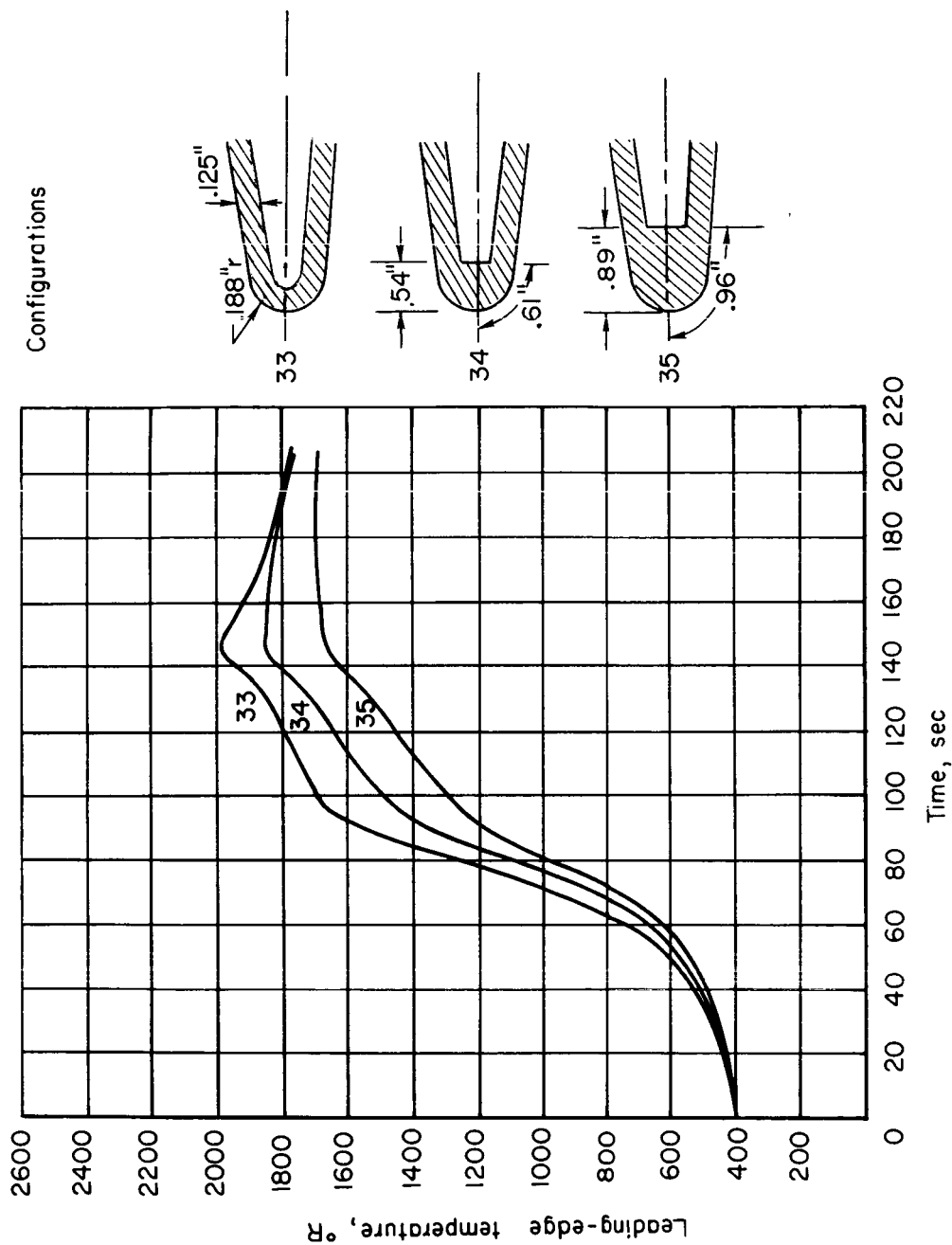
(c) Leading-edge radius = 0.188 in.; skin thickness = 0.125 in.

Figure 8.- Continued.
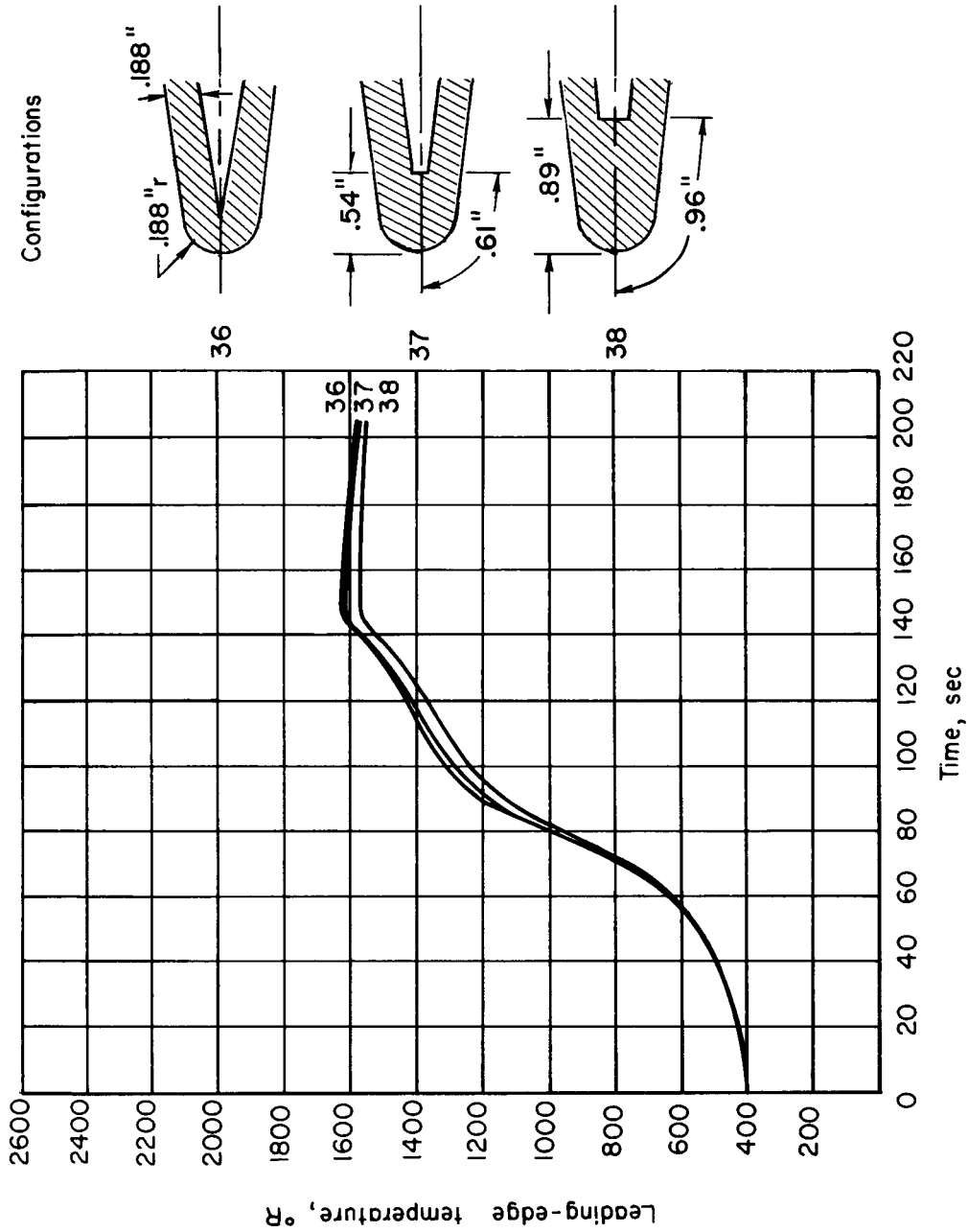
(d) Leading-edge radius = 0.188 in.; skin thickness = 0.188 in.

Figure 8.- Concluded.
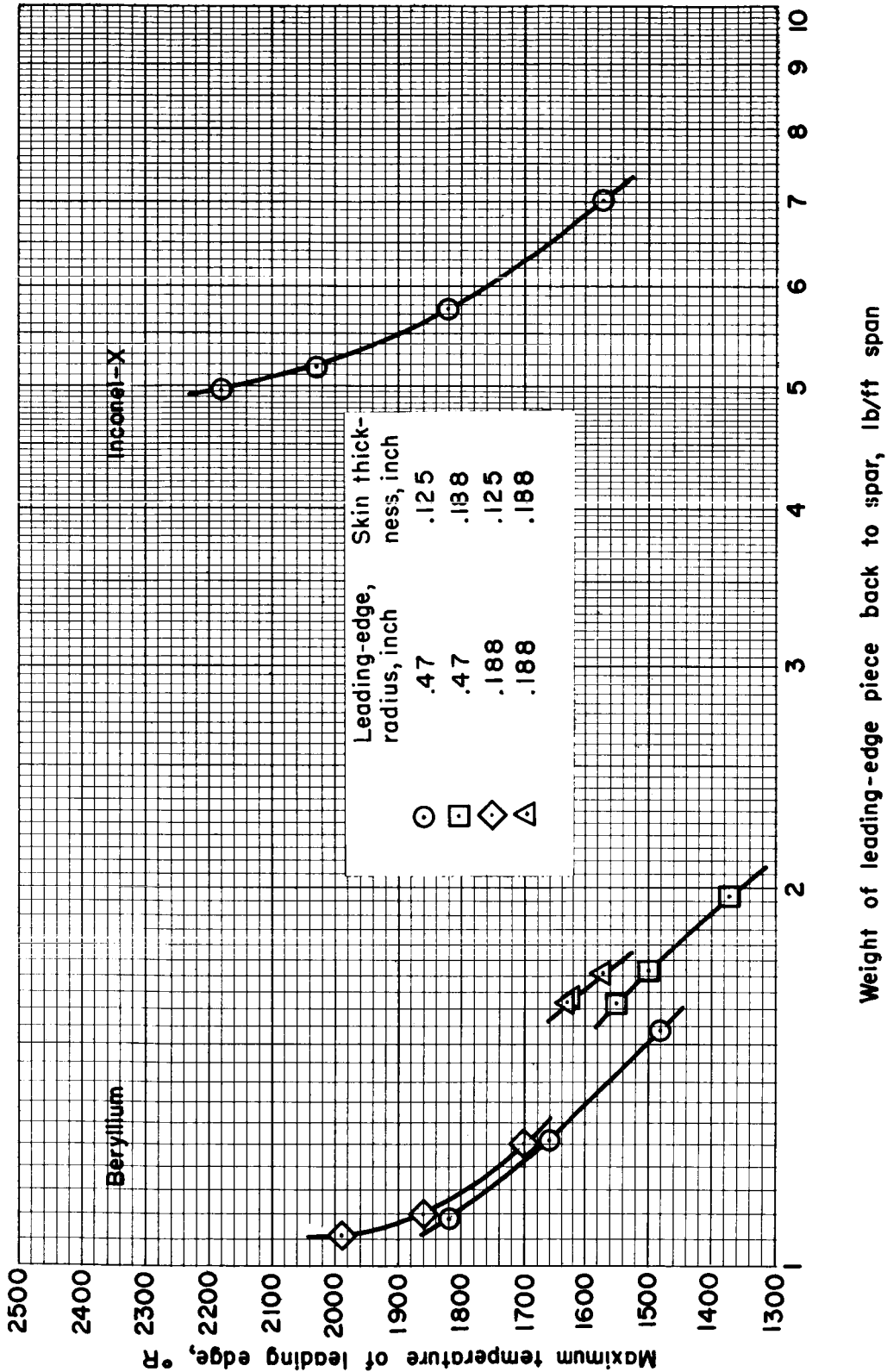
Figure 9.- Variation of maximum leading-edge temperature with weight of leading-edge piece for beryllium and Inconel-X.
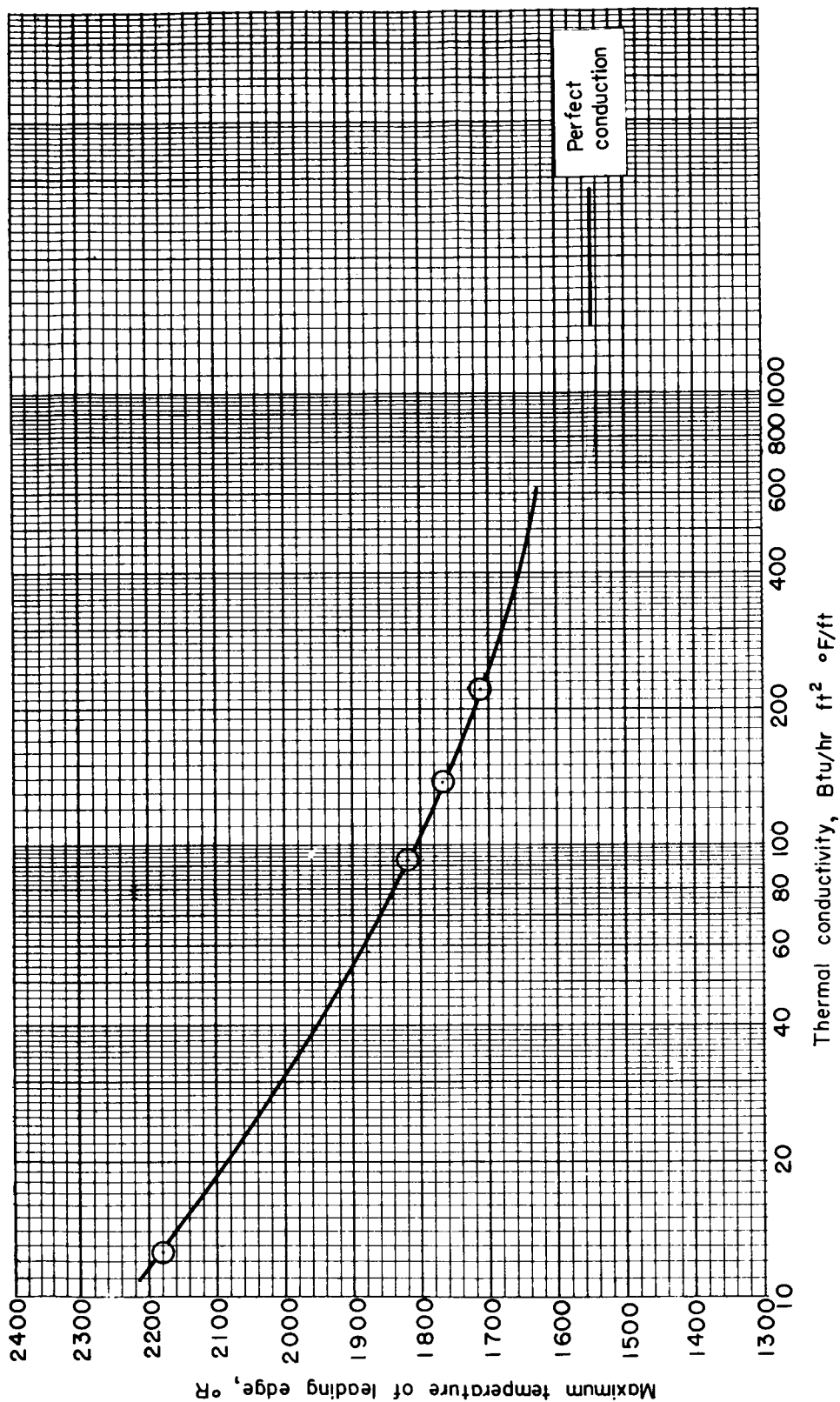
Figure 10.- Effect of variation in thermal conductivity of skin on maximum temperature of leading edge for a skin of uniform thickness and constant thermal capacity.
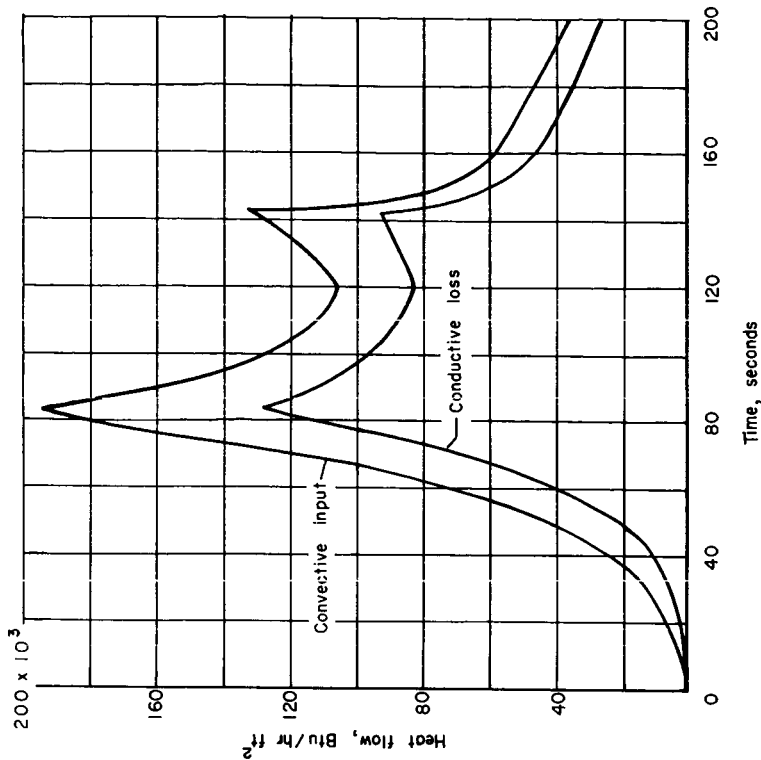
(a) Inconel-X (config. 1)
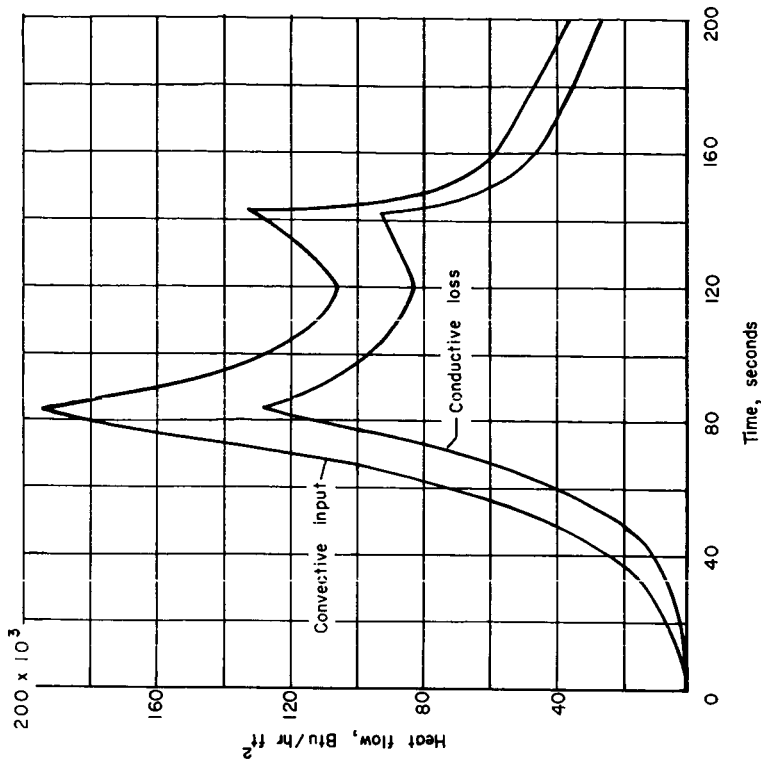
(b) Beryllium (config. 27).

Figure 11.- Calculated variation of convective heat input and conductive heat loss at leading edge as a function of time for a skin of uniform thickness.
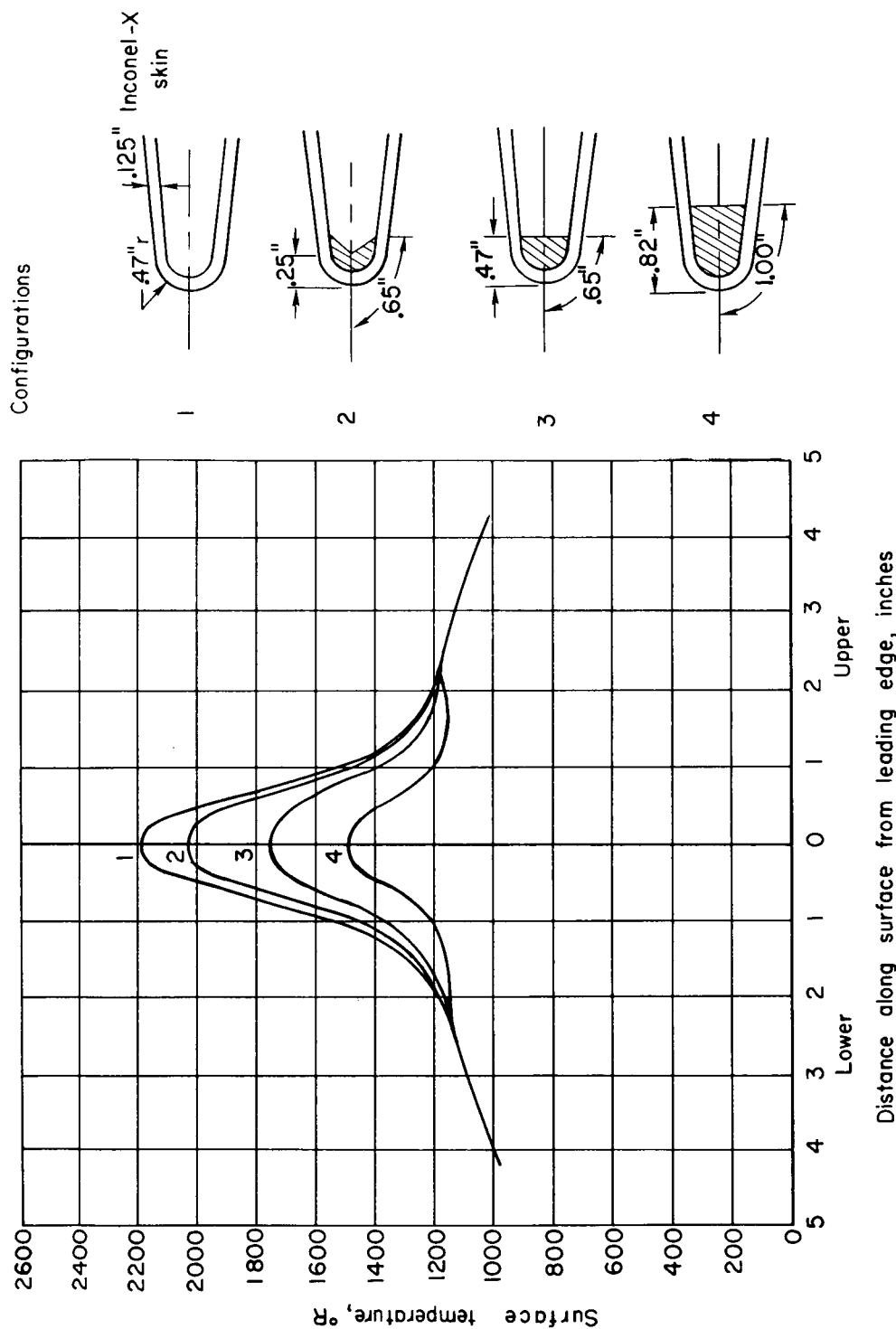
(a) Inconel-X filler material; leading-edge radius = 0.47 in.

Figure 12.- Surface-temperature distributions with various amounts of heat-absorbing material concentrated at leading edge; time = 145 seconds.

Distance along surface from leading edge, inches
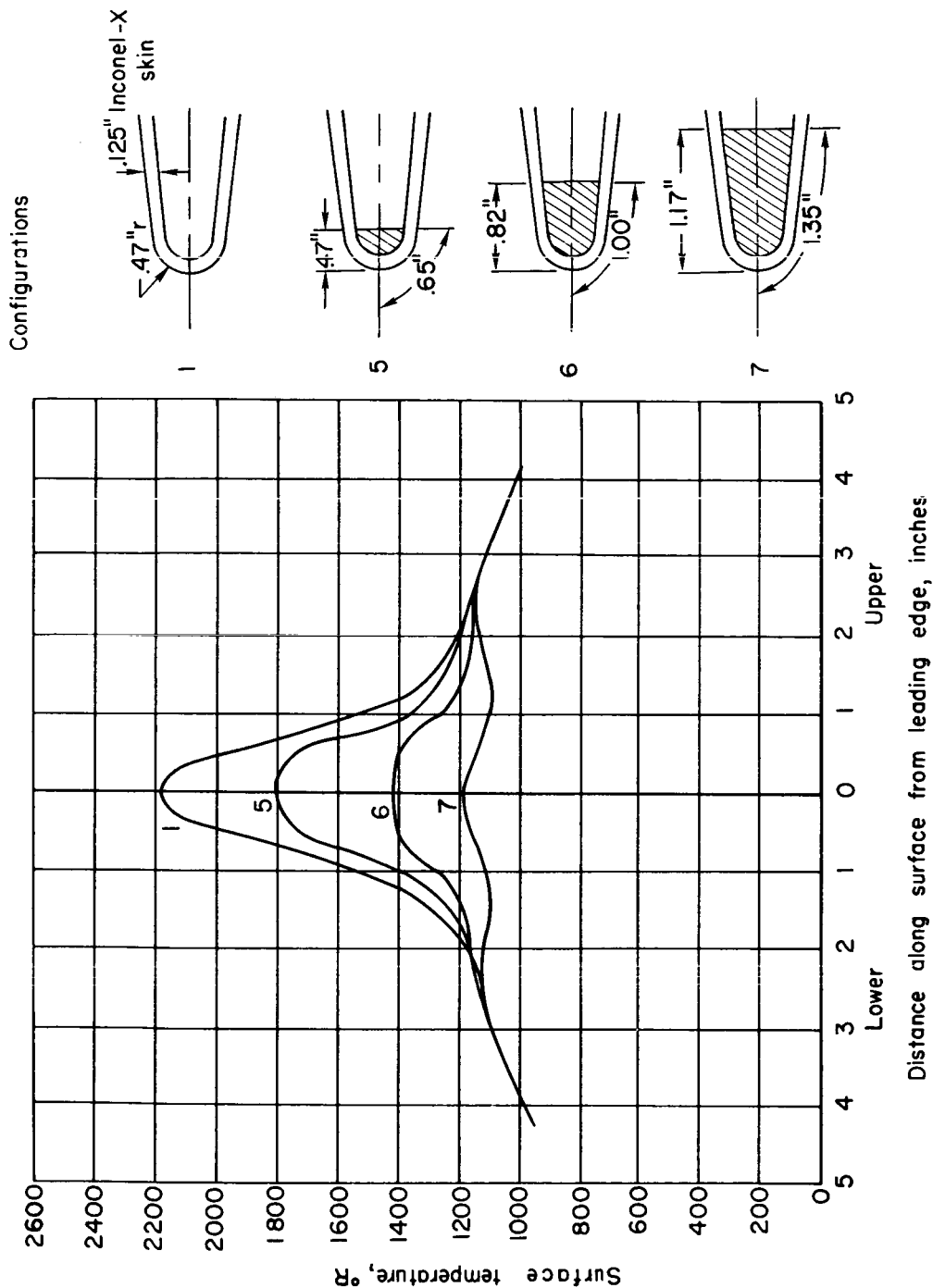
(b) Copper filler material; leading-edge radius = 0.47 in.

Figure 12.- Continued.
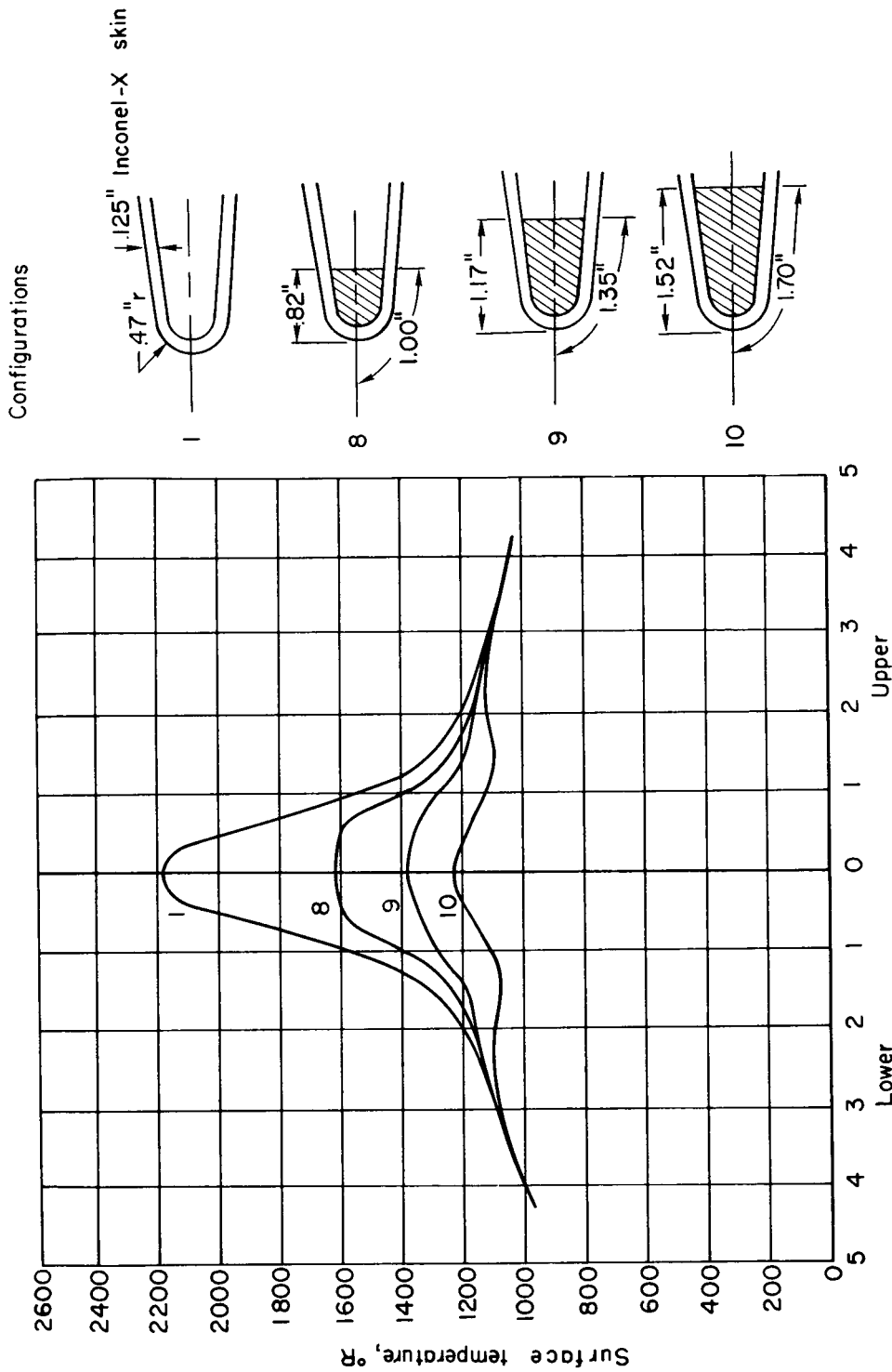
(c) Aluminum filler material; leading-edge radius = 0.47 in.

Figure 12.- Continued.

(d) Beryllium filler material; leading-edge radius = 0.47 in.

Figure 12.- Continued.

(e) Copper filler material; leading-edge radius = 0.188 in.

Figure 12.- Continued.

Configurations

Distance along surface from leading edge, inches

(f) Beryllium filler material; leading-edge radius = 0.188 in.

Figure 12.- Concluded.
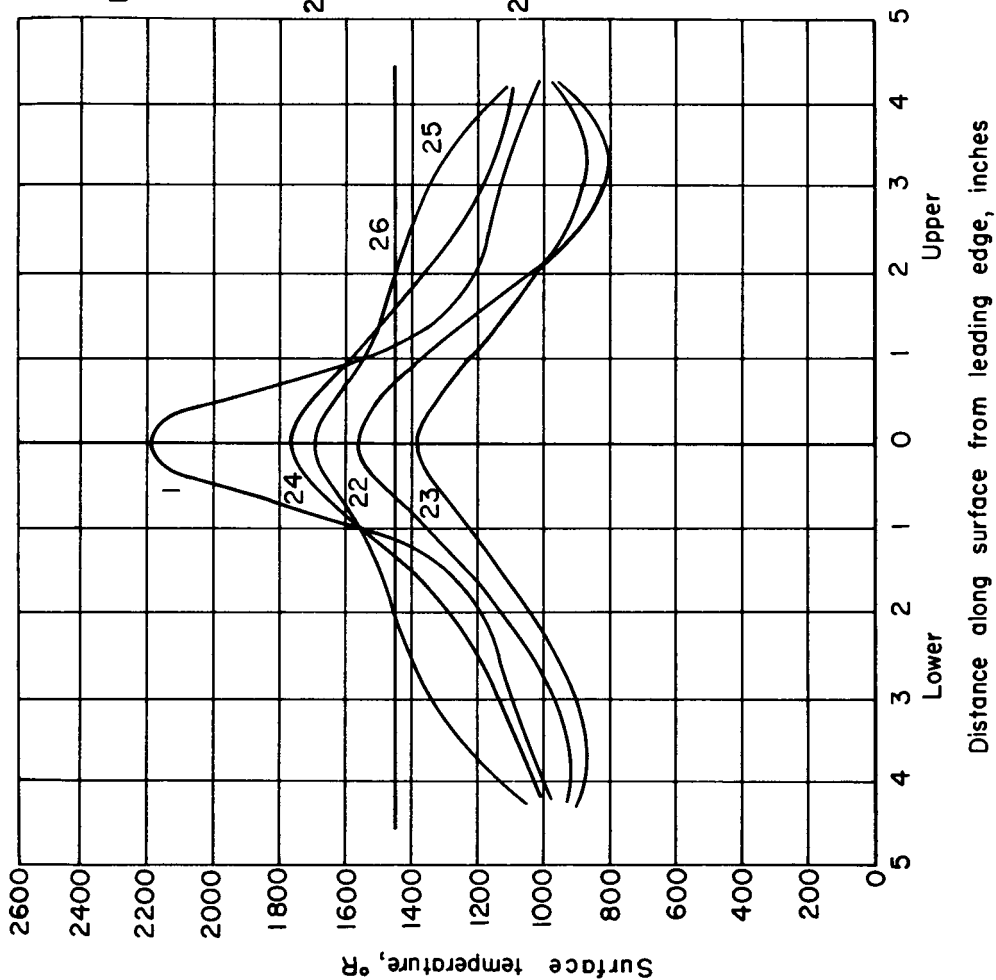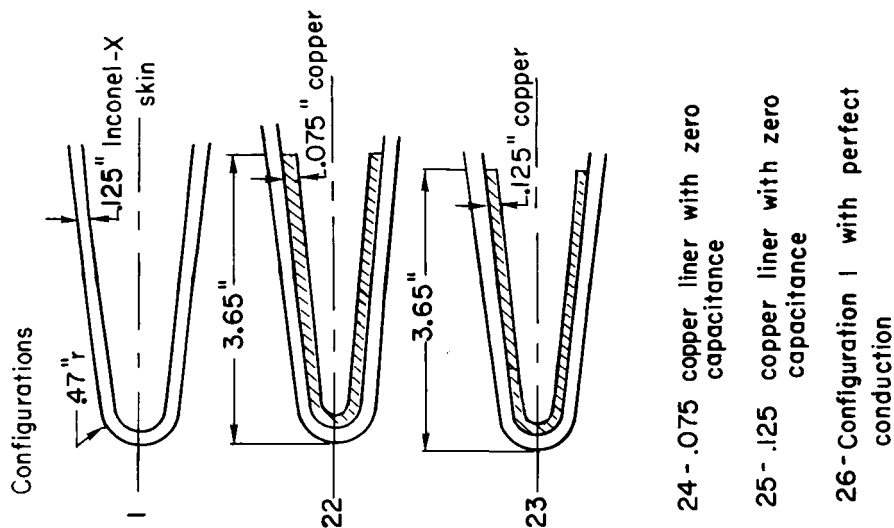
Figure 13.- Surface-temperature distributions for various arrangements of heat-conducting material distributed uniformly around interior of leading-edge region; time = 145 seconds.
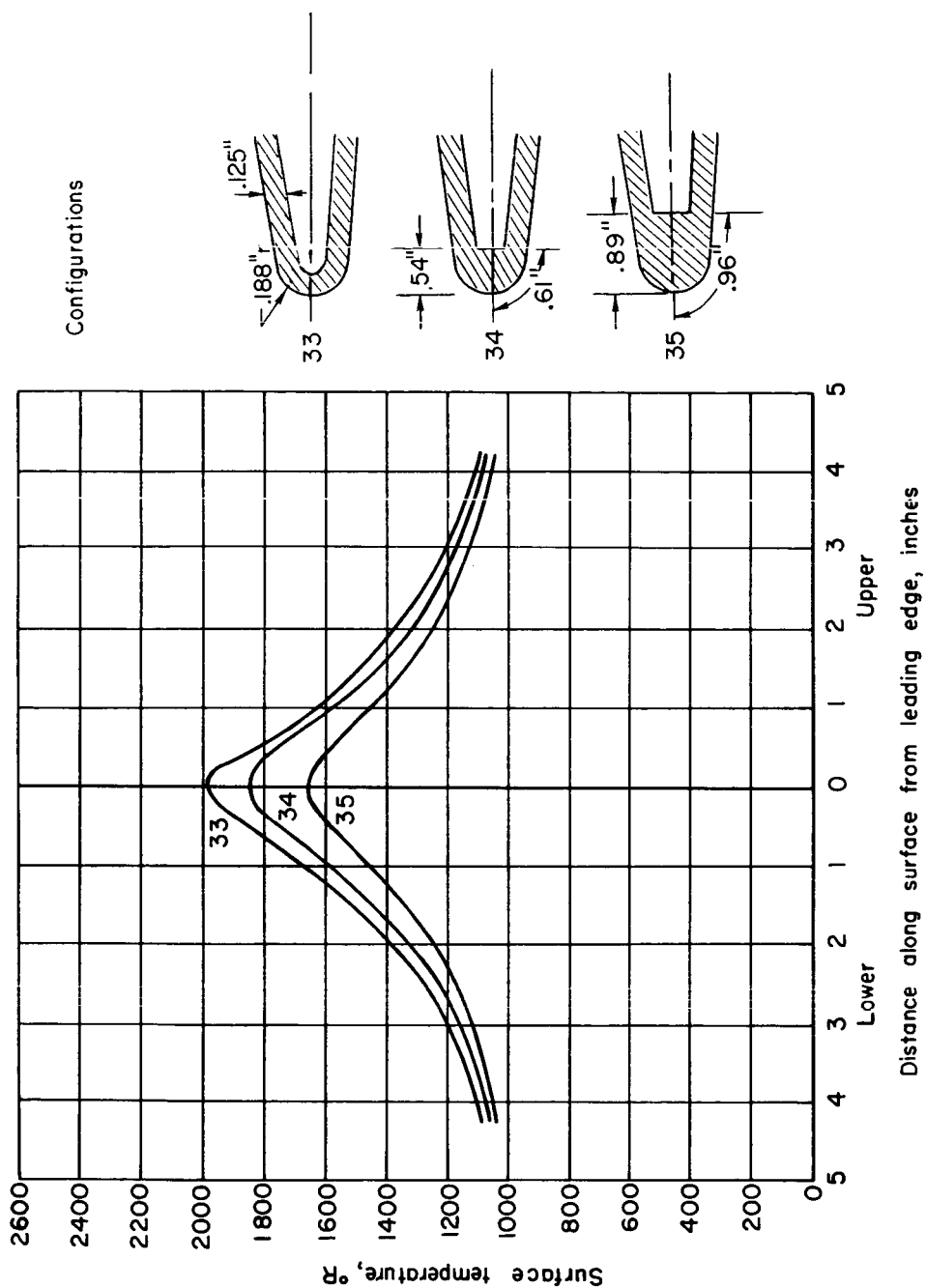
UNCLASSIFIED 45
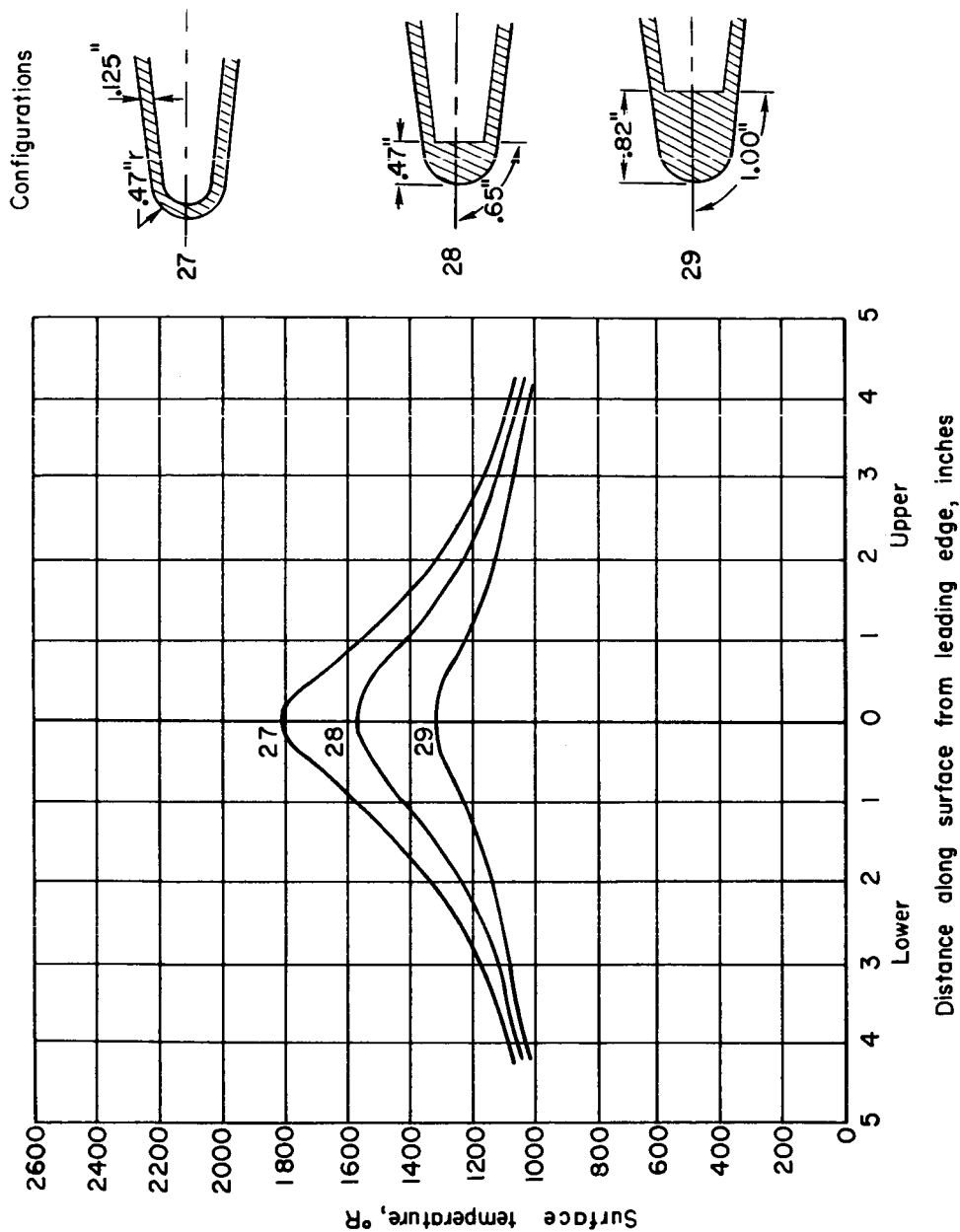
Figure 14.- Surface-temperature distributions for various configurations composed entirely of beryllium; time = 145 seconds.

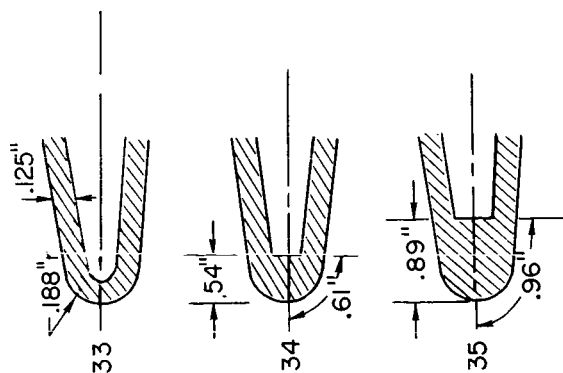(a) Leading-edge radius = 0.47 in.; skin thickness = 0.125 in.
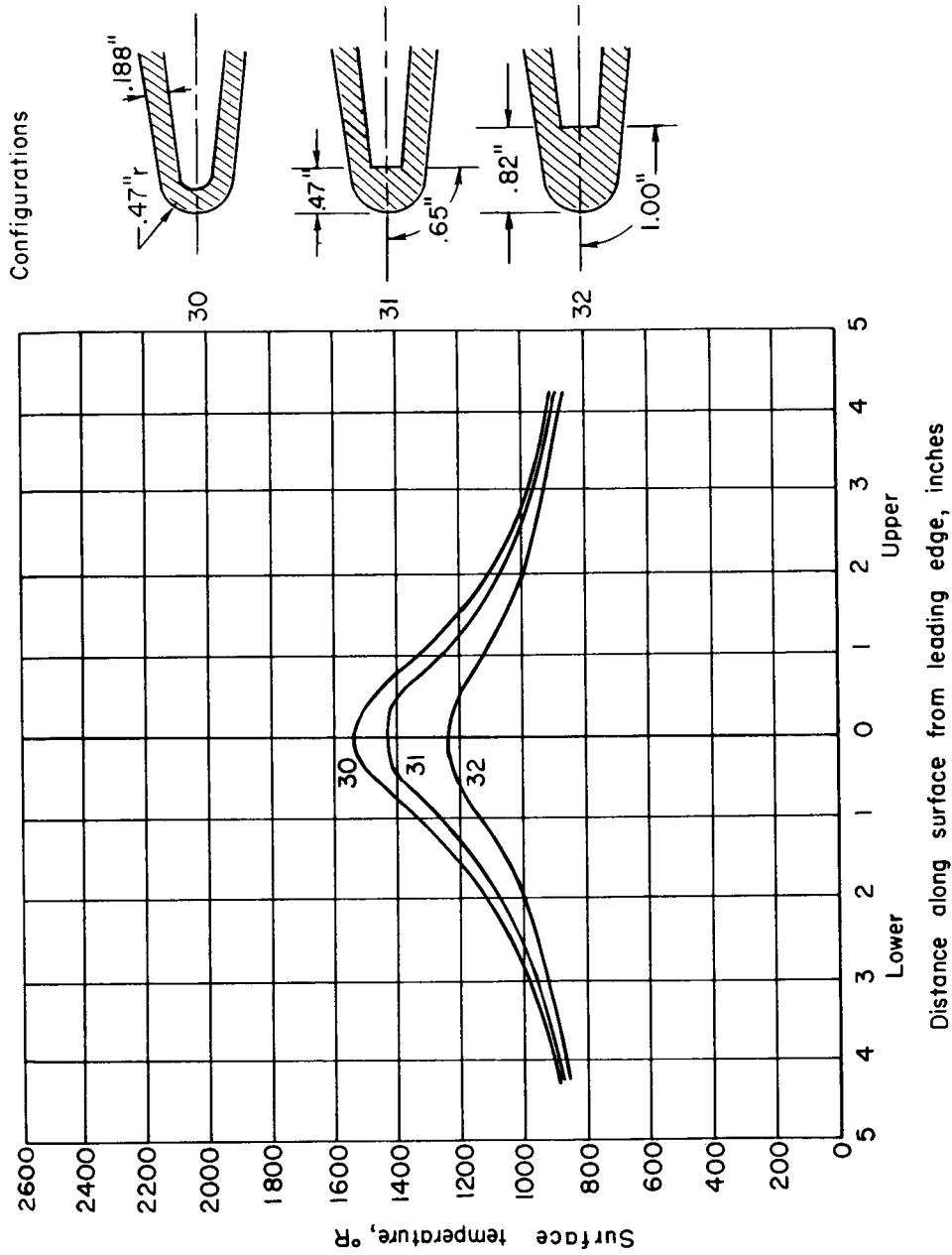
(b) Leading-edge radius = 0.47 in.; skin thickness = 0.188 in.

Figure 14.- Continued.

UNCLASSIFIED 47
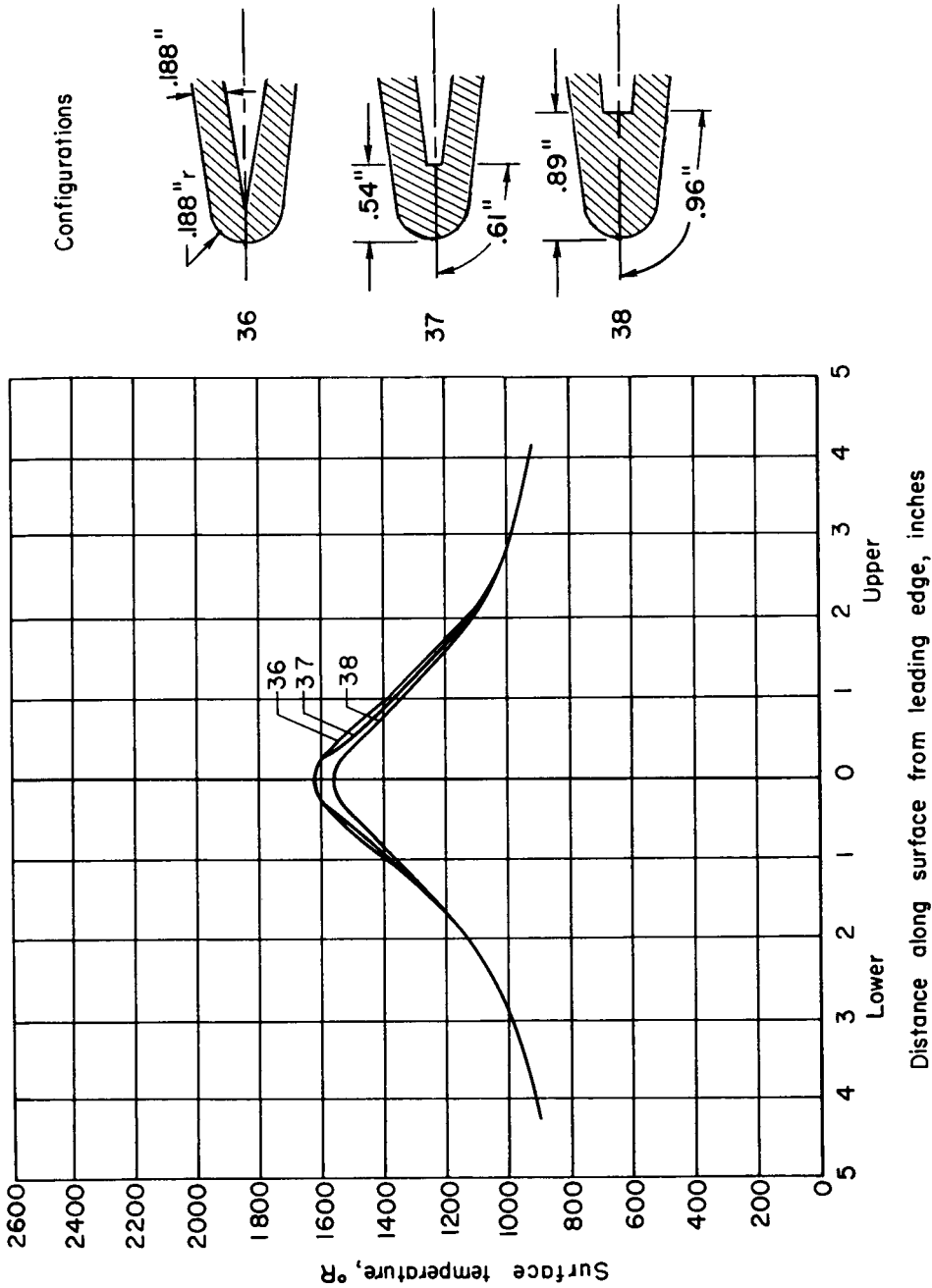

(c) Leading-edge radius = 0.188 in.; skin thickness = 0.125 in.

Figure 14.- Continued.

(d) Leading-edge radius = 0.188 in.; skin thickness = 0.188 in.
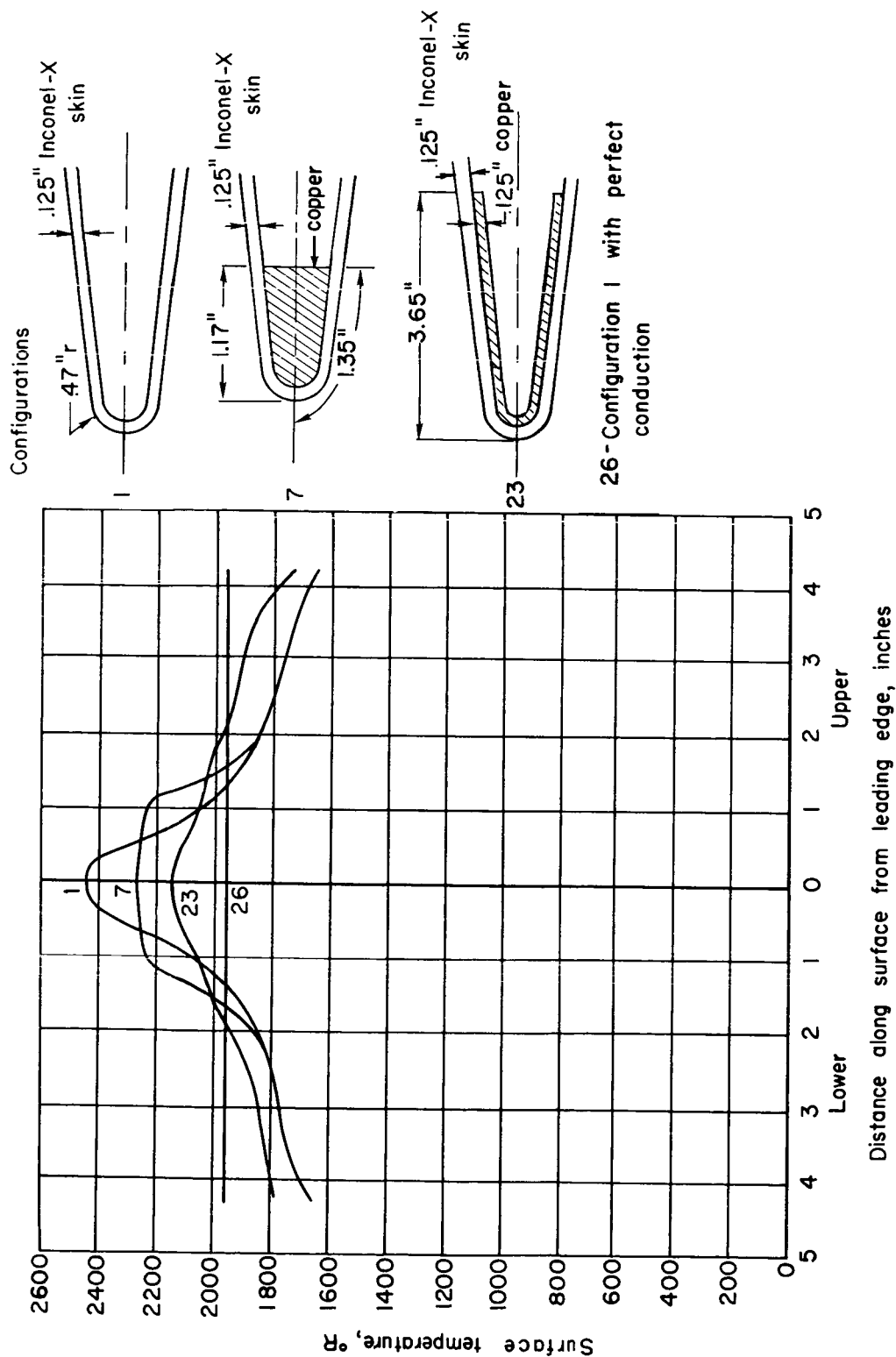
Figure 14.- Concluded.

Figure 15.- Steady-state distributions of temperature around surface of wing leading-edge region for several configurations under conditions existing at 140 seconds.